AMAZALERT Delivery Report

Title	Report on quantifying impacts of fire on climate
Work Package Number	3
Delivery number	3.3
First author	Manoel Cardoso
Co-authors	Gillian Kay, Gilvan Sampaio, Juan Pablo Boisier, Ana Paula Aguiar, Marcos Sanches, Peter Good
Date of completion	28 November 2014
Name leading Work Package Leader	G. Kay
Approved by the Leading Work Package Leader	YES / ~~NO~~

To complete by the Coordinator

Approved by the Coordinator	YES
Date of approval by the Coordinator	28 November 2014

Report on quantifying impacts of fire on climate

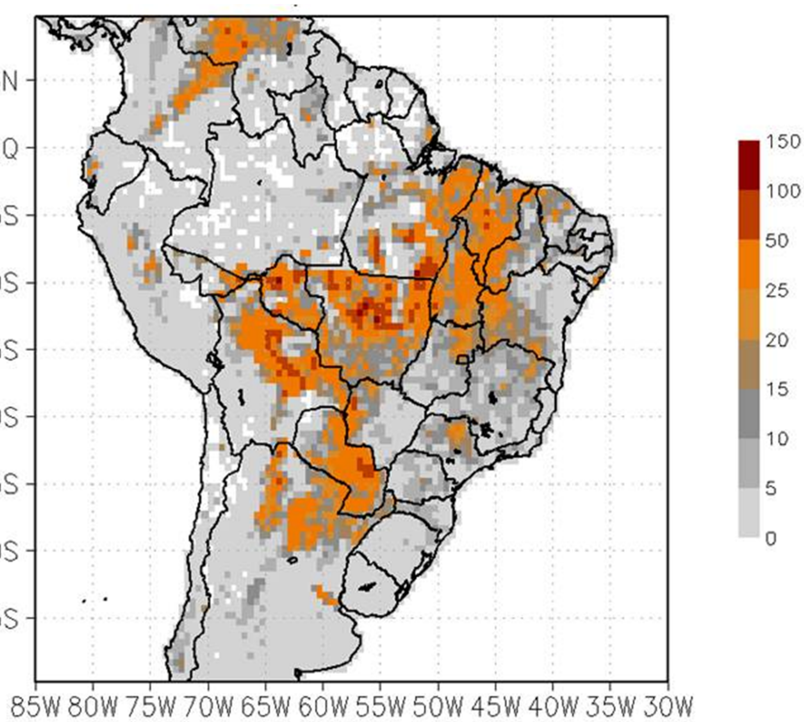

Author(s): Manoel Cardoso, Gillian Kay, Gilvan Sampaio, Juan Pablo Boisier, Ana Paula Aguiar, Marcos Sanches, Peter Good

Date: 28 November 2014

Table of Contents

Abbreviations and acronyms

AB2005	Arora and Boer (2005)
BESM	Brazilian Earth System Model
CO_2	Carbon dioxide
CMIP5	Coupled Model Inter-comparison Project Phase 5
DSL	Dry season length
ESRL	Earth System Research Laboratory
ET	Evapotranspiration
GFED	Global Fire Emissions Database
GHG	Greenhouse Gas
GOES	Geostationary Operational Environmental Satellite
GPCC	Global Precipitation Climatology Centre
HadCM3	Hadley Centre Coupled Model version 3 Carbon cycle version
HadGEM2-ES	Met Office Hadley Centre's Global Environmental Model version 2 Earth System configuration
IBAMA	Brazilian Instituto Brasileiro do Meio Ambiente e dos Recursos Naturais Renováveis
IBIS	Integrated Biosphere Model
INLAND	Brazilian Integrated Land Surface Processes Model
INPE	Instituto Nacional de Pesquisas Espaciais, Brazilian National Institute for Space Research
IPCC	Intergovernmental Panel on Climate Change
IPSL	Institut Pierre Simon Laplace, France
IPSL-CM5A	Fifth generation climate model of IPSL
LUCID	Land-Use and climate identification of robust impacts project
LW	Long wave
LuccME	Land Use and Cover Change Modeling Environment
MODIS	Moderate Resolution Imaging Spectroradiometer
MSG	Meteosat Second Generation geostationary satellite
NCEP	National Centers for Environmental Prediction
NCAR	National Center for Atmospheric Research
NOAA	National Oceanic and Atmospheric Administration
OAR	Oceanic and Atmospheric Research
PREVFOGO	Brazilian Centro Nacional de Prevenção e Combate aos Incêndios Florestais
PSD	Physical Sciences Division
RCP	Representative Concentration Pathway
RD	Surface runoff and drainage
ROLE	Outgoing long-wave radiation
SSP	Shared Socioeconomic Pathways
SW	Short wave

Executive Summary

One of the goals in AMAZALERT is to examine how changes in climate and land use will affect the Amazon region, and how these effects feed back onto climate. Fire plays an important role within these processes, due to its strong links with vegetation, climate and land-use characteristics. Fires affect biomass (Kauffman et al. 1998), vegetation structure (Cochrane and Schulze 1999), emissions of gases (Andreae and Merlet 2001), and potentially the hydrological cycle through emissions of aerosols that may lead to the formation of less-precipitating clouds (Kaufman and Fraser 1997).

Ecological long-term effects of fires are also important. While grasses are able to regrow after fires, tree mortality due to fire may prevent regeneration of woody species (Uhl & Kauffman, 1990; Cochrane & Schulze, 1999). While several factors may combine to define the boundaries between forests and savannas (Scholes & Archer, 1997; Mistry 1998), long-term biomass consumption and mortality due to fires are higher for trees than for grasses, and will potentially favour savannas in the place of forests (Bachelet et al., 2000; Daly et al., 2000; Hoffmann et al., 2000).

Fire, then, has the potential to exert considerable influence over biome distribution, but it is a process that is currently missing from most complex models. The incorporation of fire into these models is important in understanding how climate change, fire, and land cover may interact, and, in coupled modelling, will allow the operation and investigation of feedbacks within the Earth system. In AMAZALERT, we have taken some important steps in fire modelling in complex models through the implementation of a fire module in an Earth system model (HadGEM2-ES) and in a land surface model (BESM with IBIS-INLAND).

Within HadGEM2-ES, new equations estimate burned area from soil and atmospheric moisture, assuming constant rates of ignition. Plant mortality or changes in nutrients due to fires were not yet implemented, but only offline estimation of burning extent. Within BESM with IBIS-INLAND, estimation of fire potential from biomass and flammability conditions is propagated into the calculation of vegetation dynamics, which in turn affects biomass, leaf area index, and total ecosystem aboveground net primary productivity, modifying the fractional cover of forest and herbaceous canopies.

Fire equations in HadGEM2-ES were able to reproduce large-scale fire patterns, with spatial and temporal features that are similar to the patterns determined with remote sensing. Here, feedbacks between fire occurrence and vegetation dynamics were not implemented in HadGEM2-ES. Regional fire patterns estimated by IBIS-INLAND are also similar to the patterns from reference data. In the Brazilian Amazonia, fire equations in the model modify the simulation of the transitions between forests and grasslands, showing expansion of grasses over forest areas in the border between the two regions dominated by these types of vegetation.

To evaluated the combined effects of fires, climate change and deforestation, the BESM with IBIS-INLAND was run under greenhouse gas concentrations corresponding to historical conditions and scenarios of climate forcing corresponding to RCP4.5 and RCP8.5 (van Vuuren et al. 2011), and projections of land-use change for Amazonia developed by Aguiar et al. (2014). Control runs consider climate change only, and other experiments also consider fire and deforestation. In the report, we analysed results for periods 2065-2070 under RCP4.5, and 2081-2099 under RCP8.5.

For RCP4.5, model projections from BESM with IBIS-INLAND for 2065-2070 indicate warmer air temperature near the surface, compared to the control case. From the evaluation of climate change only, there is also indication of increase in annual precipitation in the south, but small change in other parts of the region. When considering deforestation and fires, the spatial patterns of the changes are the same, but the indication of decrease in annual precipitation becomes more

noticeable in the north. The estimated reduction in precipitation occurs mainly during the dry months, with increase in the length of the dry season. When considering only climate change, there is increase of upper-canopy biomass, presumably related to CO_2 fertilization. When all factors are considered, there is reduction of upper-canopy biomass and an increase of lower-canopy biomass, indicating a shift from forest to grasses.

Under RCP8.5, the results from BESM with IBIS-INLAND for 2081-2099 considering only climate change or adding fires and deforestation, are similar and indicate warmer air temperature near the surface, with the exception of the state of Acre, Tocantins, and most of the state of Para and the eastern portion of Mato Grosso. For the simulation considering all factors of change, these patterns slightly intensify and the southwest portion of the state of Acre also indicates a small cooling. The case that considers climate change and fire indicate warming near the surface in all parts of the region. For precipitation, the results considering only climate change indicate wetter conditions, with the exception of central and south portions of the region. Considering all factors there is indication of dryer conditions on the north, and considering climate change and fires there is indication of and dryer conditions on the north and eastern.

Other analyses from BESM with IBIS-INLAND under RCP8.5 for 2081-2099, considering only climate change, or all factors, indicate longer dry season in central-south portion of the state of Amazonas, in Rondonia, and in the western portion of Mato Grosso. When considering climate change and fires, the dry season is projected to be longer in most Amazonia, with the exception of the state of Tocantins, eastern Mato Grosso, southwest Rondonia and west of Amazonas. Considering only climate change, total biomass in the upper canopy is projected to increase in most of the region, and total biomass in the lower canopy is projected to decrease only in Tocantins and south of Mato Grosso. Adding fire, or deforestation and fire, the biomass in the upper canopy is projected to decrease in the north of Mato Grosso and in the eastern-northeast portion of Amazonia. In the same areas, biomass in the lower canopy is projected to increase, indicating expansion of grasses in the place of forests.

It is important to note that we expected that the results from BESM with IBIS-INLAND would present progressively stronger effects when considering changes in climate, deforestation, and fires, respectively. The results, however, show relatively small impacts of deforestation and a pronounced effect of fire. To our knowledge, these features are counterintuitive, and we plan to further investigate the sensitivity of the results to these factors and re-evaluate our treatment of the land-use scenarios in the model. We also note that these analyses were concentrated in the combined effects of fires, climate change and land use, and did not evaluate the relative strength of each of these factors. For example, we did not evaluate how much of the projected changes in biomass are due to direct land use or how much is from fire, which is also a subject for further research.

Taken together, our current results thus indicate that important changes may occur in Amazonia under the projections of future climate and land use used in this study, and the related estimates of fire occurrence linked to these projections. As shown, some portions of the region may present higher surface temperature, less precipitation, and longer dry season. An interesting feature of the results is the indication of increases in total biomass in the upper canopy when considering only climate change, probably related to the effect of CO_2 fertilization. However, including deforestation and fires some areas such as the East/Northeast portions of Amazonia show indication of important reduction in the upper biomass along with expansion of the biomass in the lower canopies, suggesting expansion of grasses in the place of forests.

1. Introduction

Each year, the cycle of fire occurrence in Amazonia builds through the dry season as meteorological conditions become more favourable, reaching a peak in September. When a dry season is longer or more intense than normal, such as during the recent drought years of 2010 and 2005, higher numbers of fires are detected via satellite monitoring systems (INPE 2014). Fires are major disturbances to vegetation and the atmosphere in Amazonia. Their effects include consumption of the aboveground biomass (Kauffman et al. 1998, Hughes et al. 2000), changes to vegetation structure (Cochrane and Schulze 1999), and emission of significant amounts of gases and aerosols to the atmosphere (Andreae and Merlet 2001). These effects also link fires to the hydrological cycle through both the influence of plants on the fluxes of water to the atmosphere, and of air composition on the characteristics of clouds (Pruppacher and Klett 1980). Fire-induced changes to the vegetation distribution modify evapotranspiration rates (Nepstad et al. 1999), while aerosols emissions lead to the formation of less-precipitating clouds (Kaufman and Fraser 1997).

Fires also have important ecological effects that can modify the establishment of forests and savannas in the tropics (Ramos-Neto & Pivello, 2000; Bond et al., 2005). While grasses are able to regrow after fires, tree mortality due to fire may prevent regeneration of woody species (Uhl & Kauffman, 1990; Cochrane & Schulze, 1999). While several factors may combine to define the boundaries between forests and savannas (Scholes & Archer, 1997; Mistry 1998), long-term biomass consumption and mortality due to fires are higher for trees than for grasses, and will potentially favour savannas in the place of forests (Bachelet et al., 2000; Daly et al., 2000; Hoffmann et al., 2000). Staver et al. (2011) argue that a large portion of the wider Amazon region could support alternative stable states of forest or savanna, and that changes brought by encroachment of fire into forest regions could be perpetuated through fire-vegetation feedbacks and result in a transition from forest to savanna.

While lightning does provide a natural source of ignition for fire, ignition points in Amazonia are generally closely related to human activity – primarily deforestation – and are reflected in the spatial expression and frequency of fire occurrence (e.g. Cardoso et al. 2003, Aragão et al. 2008). Where favourable meteorological conditions intersect with human activity, greater impacts on the forest may result from the combination of drivers than the action of either one of these. Forests that are subject to direct fragmentation or are in a more vulnerable state from changes in dry season characteristics, drought or previous fire occurrence, are more susceptible to further damage from fire when it does occur, making a shift to a different forest or vegetation type more likely (Malhi et al. 2009). Aragão et al. (2007) found that in the drought of 2005, five times the area of forest was burnt through 'leakage fires' in the Brazilian state of Acre than directly deforested, and suggest that fire leakage could be a major agent of biome change in a climate regime marked by frequent drought. Increases in temperature projected by CMIP5 and the stronger signal for a longer and deeper dry season (reported in AMAZALERT Deliverables 3.1 and 3.4) would increase the meteorological 'fire danger' particularly in the southern and eastern basin. This is the same region as projected to be subject to higher levels of land use change, and hence there is greater risk of forest loss through fire (Golding and Betts 2008; Betts et al. 2013).

Fire, then, has the potential to exert considerable influence over biome distribution, atmospheric composition and the hydrological cycle, but it is a process that is currently missing from most complex models. The incorporation of fire into these models will be an important step in understanding how climate change, fire, and land cover may interact, and, in coupled modelling, will allow the operation and investigation of feedbacks within the Earth system. In AMAZALERT, we have taken some important steps in fire modelling in complex models through the implementation of a fire module in an Earth system model (HadGEM2-ES) and in a land surface model (BESM with IBIS-INLAND). Here we present a description of the implementation procedure as well as results.

2. Previous results from CMIP5

Projections of climate change in Amazonia from the state-of-the-art CMIP5 (Coupled Model Intercomparison Project phase 5, Taylor et al. 2012) ensemble were presented in AMAZALERT Deliverable 3.1 (Kay et al., 2013) and show changes of relevance for fire occurrence and impacts in the future. Here, we set out these projections briefly to provide context for the model developments and simulations presented in Sections 4-7.

Under the CMIP5 protocol, centennial simulations have been carried out according to different scenarios of greenhouse gas (GHG) concentrations, and include land use change consistent with development pathway and policy decisions. Representative Concentration Pathways (RCPs) have been developed to describe pathways of radiative forcing and equivalent GHGs, in addition to land-use change (van Vuuren et al. 2011). Through the CMIP5 multi-model ensemble, the implications for Amazonia of following the RCPs have been explored. For the multi-model analysis, the range of RCPs was spanned through examination of changes under the low (RCP 2.6) and high (RCP 8.5) GHG pathway, as well as a 'middle-of-the-road' scenario (RCP 4.5).

There is a consistent signal for warming in the models over the 21st century, with greater warming under the higher RCPs. Maximum warming in the South America region occurs over the interior of the continent, including much of Amazonia (Figure 1). Greater temperatures are also seen during the dry season than during the wet.

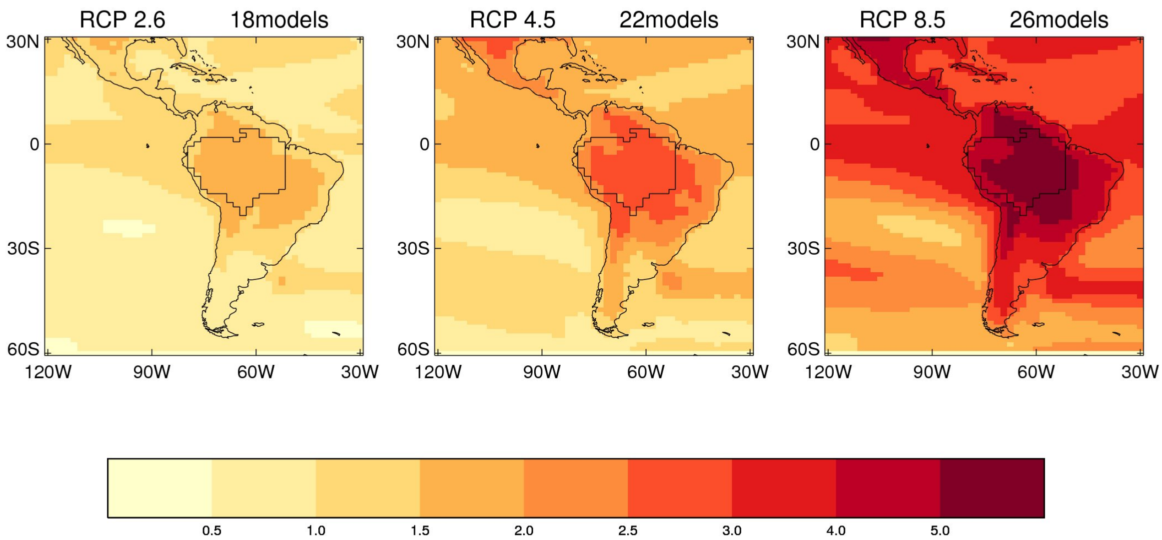

Figure 1. CMIP5 temperature anomaly projections (°C) showing the multi-model mean difference in annual temperature between late 21st and late 20th centuries for RCP 2.6 (left), 4.5 (centre) and 8.5 (right). The number of models contributing to the multi-model mean is marked above each plot.

Projections of precipitation present a more complicated picture over the Amazon basin, particularly if annual mean changes are considered. By breaking the changes down according by season and by sub-region, more consistent signals emerge, although uncertainty remains high. In the months between December and May there is a tendency towards wetter conditions, although model agreement is low. There is a stronger wet signal in the western basin and drier conditions in the eastern/northeastern basin. Between June and November, there is much stronger model agreement for drier conditions, particularly in the eastern basin (Figure 2). This points to a strengthening of the dry season, which corresponds to the current peak in fire activity.

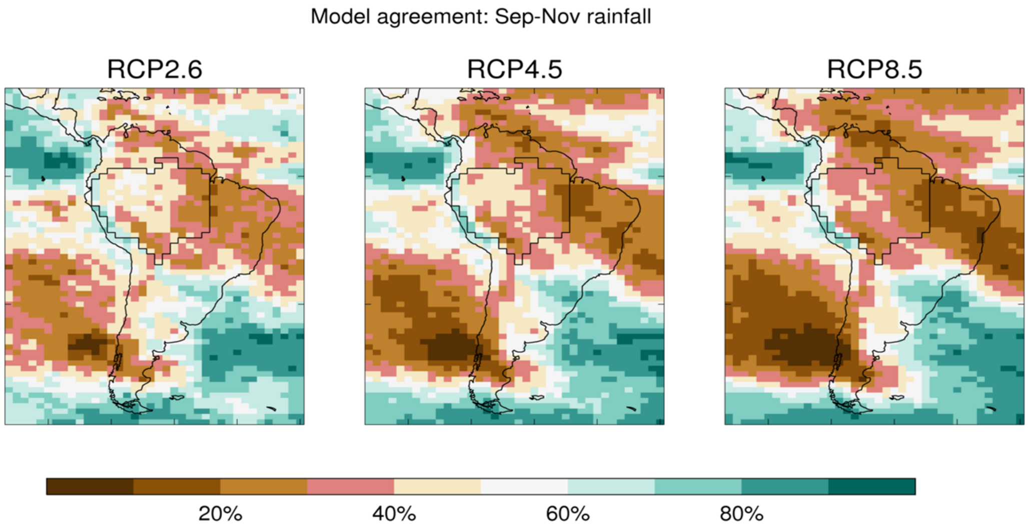

Figure 2. Indicator of model consensus in precipitation changes, September to November season. Percentage of models that show an increase in precipitation by the end of the 21st century. Brown colours indicate model agreement for a drying signal and greens for a wetting signal.

Further investigation of the CMIP5 ensemble used observations to constrain the projections. It found that compared with the direct output, the constrained projections of Amazon precipitation show a stronger signal for drying conditions, consistent with a strengthening of the South American Monsoon seasonal cycle, and a longer and more intense dry season (Figure 3). This work suggests that the standard treatment of CMIP5 output may well underestimate potential regional changes and impacts.

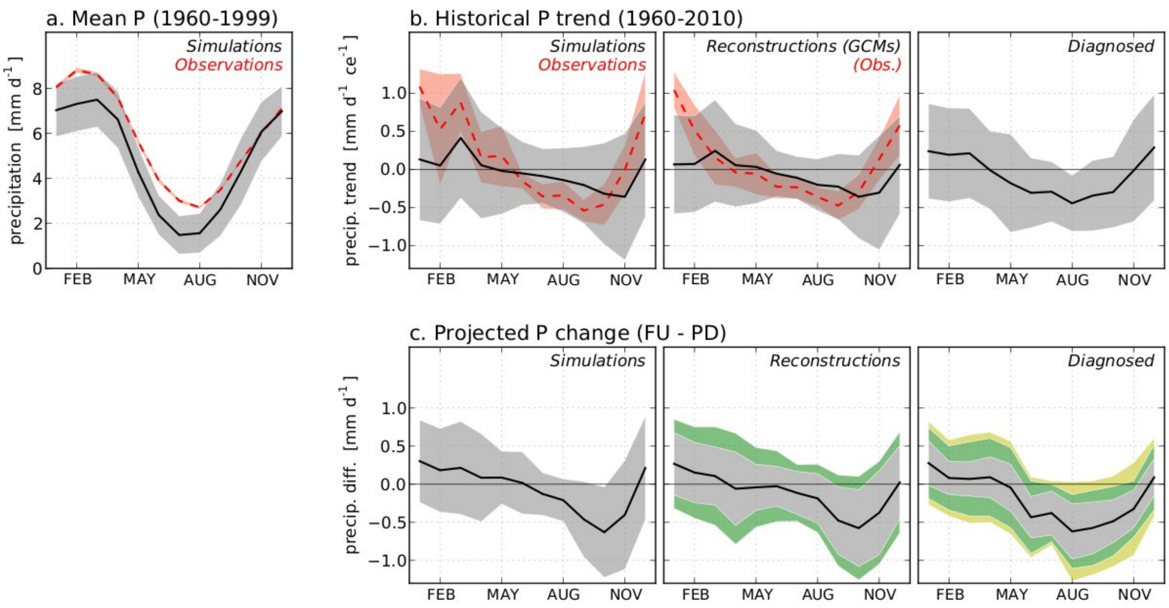

Figure 3. (a) Monthly mean present-day climatology (1960-1999) of Amazon precipitation, (b) trends from 1960 to 2010 and (c) long term precipitation change (between the ends of the 20th and 21st century). Thick lines and shading intervals indicate the ensemble mean (μ) ± 1 standard deviation (σ) of the corresponding metric of precipitation, based on GCM (black) or observational (red-dashed) data. 'Reconstructions' refer to regression models predictions in which both the input data used to calibrate the models and that used to force them are of the same origin (from GCMs or observational datasets). 'Diagnosed' refer to precipitation metrics predicted by regression models calibrated with observations and forced with large-scale motion indicators

simulated by GCMs. Light grey shades in the diagnosed precipitation metrics indicate the contribution to the overall σ associated with uncertainty in observations. From AMAZALERT Deliverable D3.4, Kay et al. 2014, their Figure 7, and updated in Boisier et al. (*submitted*).

3. Monitoring and modelling fire and its impacts

3.1. Monitoring

For large regions such as Amazonia, most of daily to monthly information on fire activity and extension are from satellites, because of their ability to cover large regions in relatively short periods of time. They can map temperature and changes on the land surface, and help to estimate fire occurrence and extent on vegetated surfaces. In common with other remote-sensing products, fire detections from satellites also present uncertainties that are worth to note (Schroeder et al. 2008). For example, clouds and tree canopies may hide fires from satellites, and very reflective surfaces may be confounded with burning spots. Fires happening before or after sensors overpass can also cause omission errors. Taken together, omission errors are more likely than commission errors in fine-scale fire detections for Amazonia (Cardoso et al. 2005). At the relatively large spatial and temporal scales of our analyses, however, remote sensing provides information that are in good agreement with knowledge from the ground. As an example, fire activity and risk are monitored daily at INPE based on detections from geostationary (GOES, MSG) and polar-orbiting (AQUA, TERRA, NOAA) satellites. Together with data on precipitation, temperature, relative humidity and vegetation cover, this system provides information that help preparedness and emergency decisions for other institutions preventing catastrophic fire events in protected areas in Brazil, such as the National Center to Prevent and Combat Forest Fires (Centro Nacional de Prevenção e Combate aos Incêndios Florestais PREVFOGO/IBAMA) (INPE 2014).

To develop and test models in this project, we have used remote-sensing information from active-fires and burned-area products for years 2001-2010. Active-fires data are from the Moderate Resolution Imaging Spectroradiometer (MODIS) Collection 5 Active Fire Product (Giglio 2013) (Figure 4), and information on burned area are from the Global Fire Emissions Database (GFED) (van der Werf 2010). These datasets were selected based on their spatial and temporal coverage and level of detail, complete documentation, good record of publications and previous applications in other studies for the study region.

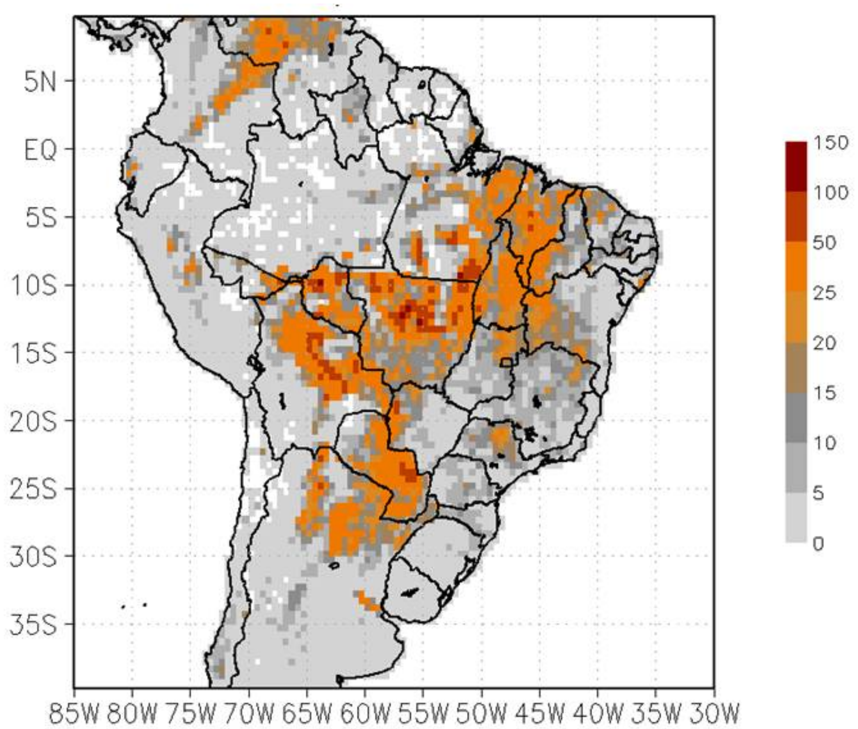

Figure 4. Fire detections from MODIS. The map shows the average monthly fire detections between 2001 and 2011. Source: National Atmosphere and Space Administration (NASA).

3.2. Modelling

Fire models are important tools for synthesis and projections, reflecting the knowledge obtained from observations made on the ground or by satellites, and enabling the evaluation of future fires in response to scenarios of land surface and climate. At the spatial and temporal scales of climate and ecosystem models, fire dynamics are normally represented by equations that consider major factors for fires, such as presence of fuel, flammability and sources of ignition. Globally, these variables are normally related to above-ground biomass (fuel), precipitation and relative humidity (flammability), and lightning and changes in land cover and use (sources of ignition).

In Amazonia, at monthly to yearly temporal scales, most fires are linked to a combination of factors related to climate and land-use activities (Cardoso et al. 2003, Cochrane 2003). Within the scope of AMAZALERT, we have evaluated the application of previous methods for estimating fire occurrence and effects, and selected the fire model developed for the Canadian terrestrial ecosystems model CTEM (Arora and Boer, 2005), and the work of Kasikowski et al. (*in prep.*) initially developed for the HadCM3 general circulation model developed at the UK Met Office Hadley Centre. These models were selected based on their suitability for global applications, they can operate at scales that are useful for the intended analyses, and calculate variables that are of interest for fire research.

4. Role of Land Use: historical and future

Recent model intercomparison studies, such as those resulting from the LUCID (Land-Use and Climate, IDentification of robust impacts project) initiative, have shown that the scenarios of land-use (LU) changes used by the CMIP5 models have had very little impact on the climate (Brovkin et al., 2013) of Amazonia. For the Amazon basin, the scenarios of LU are in most cases very optimistic and do not reflect the present-day rates of deforestation (see AMAZALERT deliverable D3.1). The lack of realistic land-cover forcings for the Amazon responds both to deficient characterizations of regional (country-level) socioeconomic processes driving changes in LU in large-scale land-cover datasets, and to inadequate interpretations of those datasets when adapted in land-surface models (de Noblet-Ducoudré et al., 2012).

Under AMAZALERT, new scenarios of land use change have been developed (Aguiar et al. 2014, AMAZALERT Deliverable D4.2) using the LuccME modelling framework (available at http://www.terrame.org/luccme). These describe three contrasting scenarios of change (Figure 5) that sample low to high environmental and social development futures, aligned with the IPCC Shared Socioeconomic Pathways (SSPs). These regional LU scenarios should be more appropriate to perform regional-scale analyses than the LU scenarios used in the simulations of CMIP5.

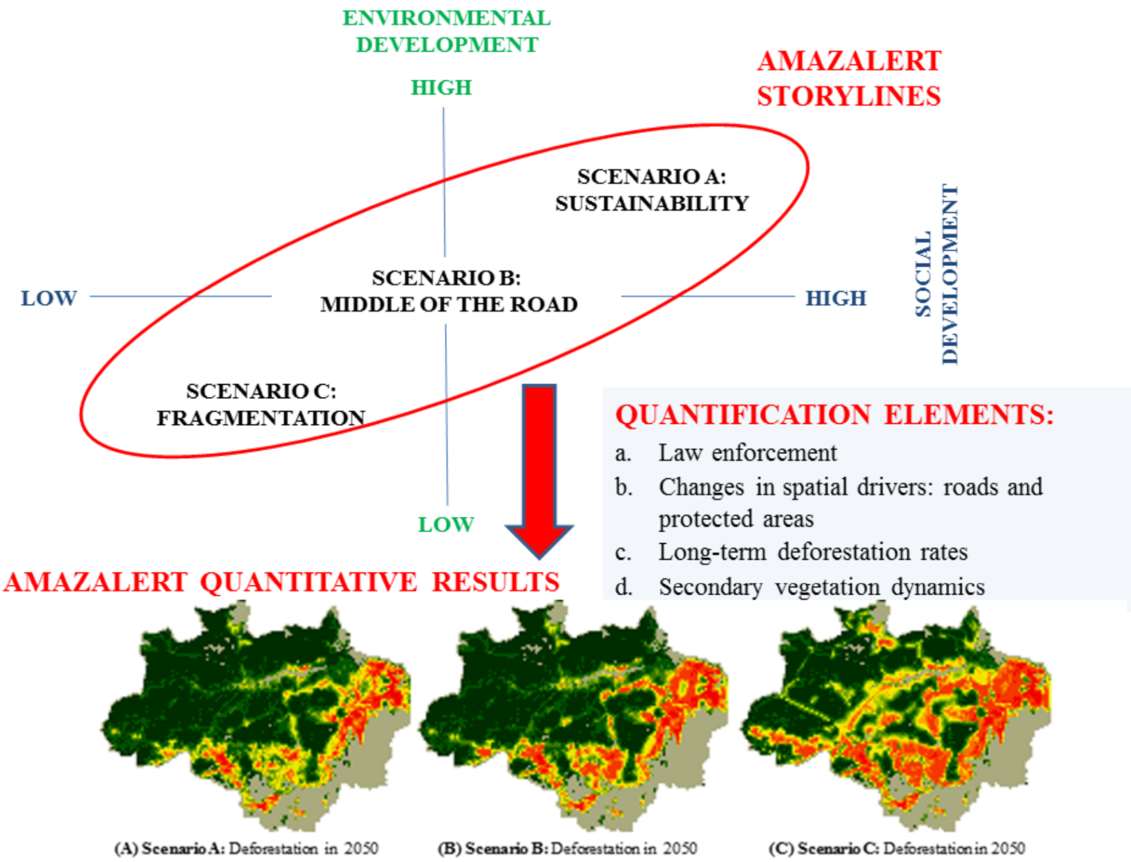

Figure 5: The three scenarios of land use change developed by AMAZALERT. Figure courtesy of Aguiar et al. 2014, AMAZALERT D4.2, their Figure 3.

The most severe LU scenario projected to 2050 by LuccME (Scenario C, the so-called ‘Fragmentation Scenario’, hereafter referred to as LuccMEc) was implemented in modelling experiments by WP3 partner institutes to evaluate the potential impacts in Amazonia under this scenario, and to provide a comparison with the low land-use change in the standard CMIP5 experiments.

As a basin average, the IPSL-CM5A model simulates a positive annual precipitation trend in response to the standard RCP8.5 forcing (Figure 6), while HadGEM2-ES simulates decreasing precipitation. These regional signatures of climate change place these two models towards either ends of the CMIP5 ensemble range (Kay et al. 2013, AMAZALERT Deliverable D3.1). Changes in the other components of the hydrological cycle – evapotranspiration (ET) and in surface runoff and drainage (RD) – are consistent with changes in precipitation within the two models.

The IPSL-CM5A model was run out to 2050 under CMIP5 RCP8.5 conditions, but with LuccMEc LU in the Amazon basin. The 'LU-induced effect' was computed as the mean difference between LuccMEc and the standard RCP8.5 at the end of the period simulated (2035-2050). It shows the effect of the new LU scenario over the standard forcing, and is illustrated for each component of the surface water budget on the right hand panels of Figure 6. Although the LuccMEc simulations still show basin-average increases in precipitation, ET and RD, the relative effect of the new LU is for statistically significant decreases in these quantities in many areas of the basin. This finding is consistent with previous modelling work that suggested that large-scale deforestation could bring about reductions in precipitation (Sampaio et al. 2007) and also some observational evidence (Spracklen et al. 2012). The amplitudes of the changes are generally lower than but of the same order as those induced by the greenhouse gas forcing. Hence, on average across the Amazon, the hydrological impacts of large-scale climate change, as simulated by IPSL-CM5A, are significantly damped by the LU effects.

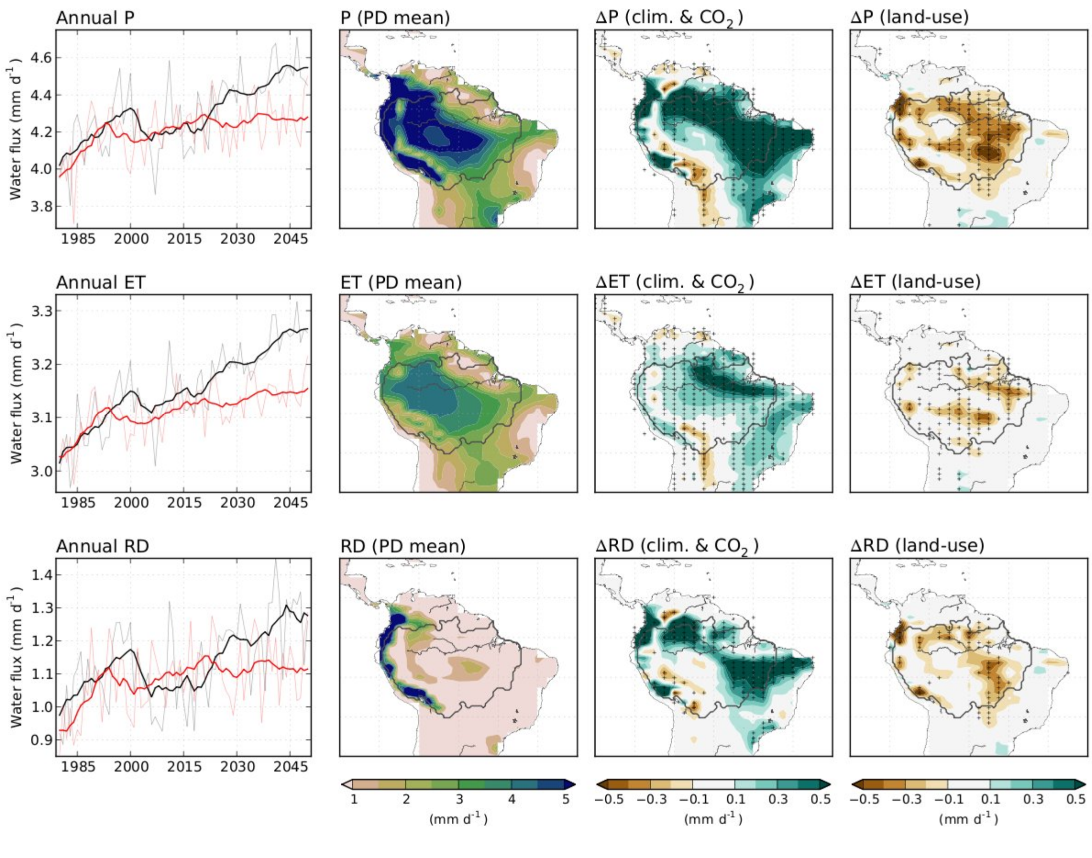

Figure 6. Amazon basin-average times-series of annual precipitation (top), evapotranspiration (middle) and runoff/drainage (bottom), from simulations S1 (black) and S2 (red). The ensemble and 5-yr moving average is indicated as thick lines. The maps illustrate, for each variable, the present-day (1980-1995) climatology (centre-left), and the long term change driven by GHGs (centre-right) and land-use (right). Marks indicate the anomalies that are statistically significant ($p < 0.05$). Figure presented also in Kay et al. 2014, AMAZALERT Deliverable 3.4, their Figure 9.

Additional experiments were carried out using HadGEM2-ES, in which the standard RCP8.5 at 2050 was compared as a 'time-slice' with another simulation, identical except for the LuccMEc 2050 LU imposed within the Amazon basin. Consistent with the IPSL-CM5A results, the additional deforestation has a drying effect in Amazonia in comparison with the standard RCP, with reductions seen in precipitation, ET and RD relative to the global climate change-driven effects. In looking more closely at deforestation-induced changes in ET, the basin was divided according to dry season length (DSL, rainfall >100 mm month^{-1}, after Sombroek 2001), as a measure of variation in forest-relevant underlying environmental conditions (Figure 7). DSL in HadGEM2-ES has been used elsewhere to calculate a descriptor of tropical forest distribution (Good et al. 2013). The response of the model was analysed for three regions defined by DSL: 0-2 months, 2-4 months, 4-6 months, the first region being the wettest and the last the driest. Short dry seasons are found in the north-west portion of the basin, with longer dry seasons towards the south and east.

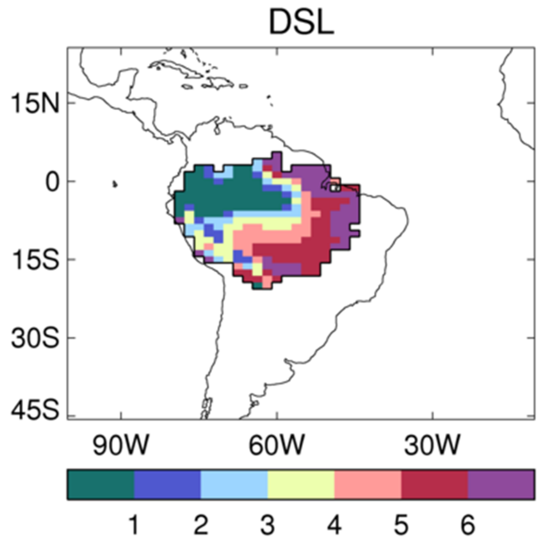

Figure 7. Dry season length in months as simulated by HadGEM2-ES. This is used to divide the Amazon basin for further analysis.

The response of the model to deforestation is different according to the underlying state: In regions marked by a short dry season, i.e. where conditions are wetter, the effect of deforestation on ET is much smaller than in regions where there is a long dry season, in the south and east. Figure 8 illustrates the effect of the loss of trees on the seasonal cycle of ET, according to DSL region. The right-hand figure shows the regression relationship between changing forest fraction and ET. Positive numbers indicate a decrease in ET with reduction of broadleaf trees. This demonstrates that largest effects of deforestation are seen during the dry season and in regions that are already characterised by long dry seasons, in the south and east.

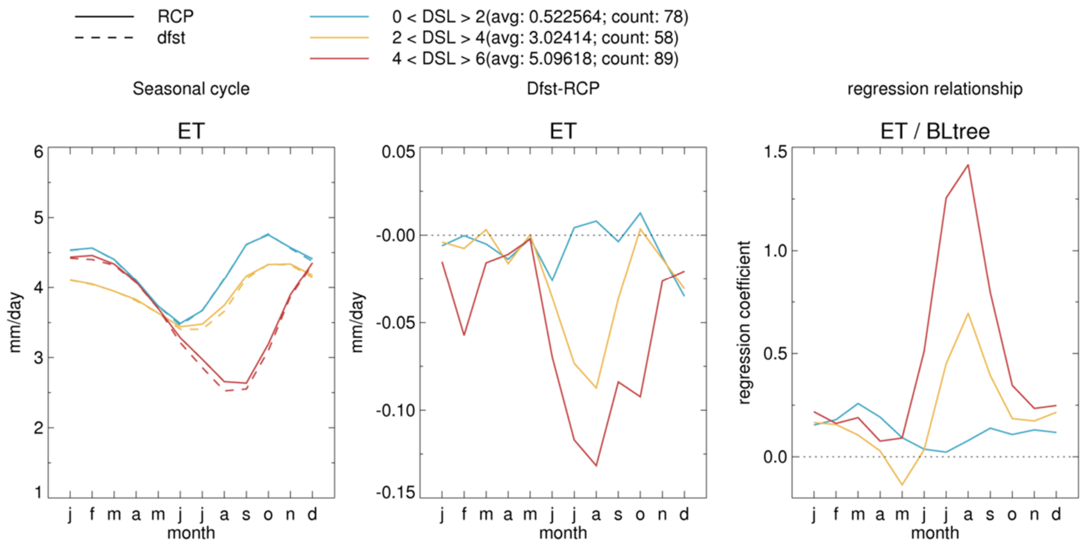

Figure 8. Effects of loss of trees on the seasonal cycle of evapotranspiration (ET) in Amazonia, by dry season length (DSL) region: 0-2 months, blue; 2-4 months, yellow; 4-6 months, red. In brackets are shown the

average lenth of dry season within each region, and the number of model grid cells contribution to the calculation. Left: seasonal cycle in the standard RCP (solid line) and LuccMEc run (dashed line); Centre: difference between LuccMEc and RCP; Right: regression relationship between the change in forest fraction and change in ET.

The results from both sets of experiments indicate that loss of forest in the Amazon basin has a drying effect on the regional hydrology, with potential implications for ecosystem service provisioning, and also in altering the conditions towards a state more favourable for the spread and intensity of fire. Results from the analysis of the standard CMIP5 ensemble (Kay et al, 2013 AMAZALERT Deliverable D3.1; Joetzjer et al. 2013) and projections from the ensemble constrained by observations (Boisier et al. *submitted*; Kay et al. 2014, AMAZALERT Deliverable D3.4) have reported a tendency towards an expanding dry season, in length and in extent, which again would enhance fire susceptibility. These results underline the need to combine these effects with a fire model to assess the impacts on Amazon biomass. In Section 7, there are some results combining these effects to assess the impacts on Amazon biomass.

5. Implementation of fire module within BESM and HadGEM2-ES

5.1. BESM

As part of the Brazilian Earth System Model (BESM, Nobre et al. 2013), a new model is being developed to represent global land processes with emphasis in ecosystems in Brazil, named Brazilian Integrated Land Surface Processes Model (INLAND, http://www.ccst.inpe.br/inland). INLAND derives from the Integrated Biosphere Simulator (IBIS) (Foley et al. 1996, Kucharik et al. 2000), and in in the context of this work, it is referred to as IBIS-INLAND. The model has been improved to represent the major features of the fire occurrence with emphasis on the ecosystems in Brazil, based on the method developed by Arora and Boer (2005) (AB2005). At this stage, the development and implementation of the fire model is concentrated on the simulation of fire probability and effects on vegetation dynamics only. For that, we implemented the fire occurrence probability equations of AB2005, where fire potential is driven by the combination of presence of fuel, flammability, and sources of ignition.

Presence of fuel is represented as in AB2005, which stipulates that a minimum of 200 gC/m^2 of plant biomass is required to sustain a fire. In the Inland implementation, plant biomass was considered as the sum of stem and leaf biomass from all vegetation types over land. Flammability, as described in AB2005, increases exponentially as soil moisture at the root zone approaches the wilting point. In Inland, we calculate flammability based on the moisture at the model's first soil layer, where most roots are located. Our approach to represent sources of ignitions differed from AB2005 in our assumption that ignition processes are simply random. Final fire occurrence probability is calculated by multiplying these three estimates, as in AB2005.

To account for fire disturbance, we propagated the estimation of fire potential into the calculation of vegetation dynamics, following the current formulation of Inland for considering disturbances. That was done by assuming that the fraction of the vegetation affect by fires is proportional to the fire probability. As for other disturbances, Inland considers that fire disturbance (fraction of affected vegetation by fires) affects biomass, leaf area index, and total ecosystem aboveground net primary productivity, which in turn modify the fractional cover of forest and herbaceous canopies.

5.2. HadGEM2-ES

The fire model implemented in the Hadley Centre Global Environmental Model version 2 (HadGEM2-ES, Collins et al. 2011), is based on the work of Kasikowski et al. ("Development and optimisation of a scheme for simulating burnt area in a climate model") initially designed for the Hadley Centre Coupled Model version 3 (HadCM3). The model estimates burned area for each class of vegetation considered by the model, from soil and atmospheric moisture, assuming constant rates of ignition.

The original HadCM3 equations were re-parameterized to accommodate the increased HadGEM2 spatial resolution, using reference burned area information from the GFED dataset for years 2001-2010, and atmospheric and soil moisture information from HadGEM2-ES AMIP run for 1994-2008. All data were aggregated as monthly climatologies, resulting in a model tuned to reproduce monthly climatological burned area.

It is important to note, however, that the fire model within HadGEM2-ES does not yet represent feedbacks between fire occurrence and vegetation dynamics. So, there is not, at this point, implementation of plant mortality or changes in nutrients dynamics due to fires, but only offline estimation of burning extent.

5.3. Implementing different fire types

Although the direct relationships between deforestation and fires were not explicitly represented in the model equations, in Inland, we also included the related effect of deforestation processes as an increase in the disturbance rates for the vegetation in Amazonia. Based on a similar approach used for fire, deforestation processes were considered in Inland by accounting for this disturbance when calculating the dynamics of the vegetation. In this case, no additional assumptions were made, and input deforestation data were assimilated by directly interpreting it as a fraction of affected vegetation. For deforestation, we assume that the grid-cell fraction of vegetation affected by deforestation only impacts tropical, temperate and conifer broadleaf, evergreen and deciduous trees. For these classes, deforestation changes plant biomass, leaf area index and net primary productivity.

6. Model validation

6.1. IBIS-INLAND

The new implementations of fire occurrence and effects in the model were tested in simulations where the model was run for a total of 699 years (1400-2099), to allow for equilibrium of the slow carbon pools and to test the model stability. There was an initial spin-up period of 366 years (from 1400-1765) under constant pre-industrial atmospheric CO_2 concentrations (278 ppm). The runs were continued from 1766 to 2005 with increased prescribed atmospheric CO_2 concentrations (from 278 to 378 ppm), and from 2005 to 2099 with atmospheric CO_2 concentrations following the Coupled Model Intercomparison Project 5 (CMIP5) protocols. From 1400 to 2005, climate data was applied cyclically, and after 2005 from CMIP5 models. The results presented here represent only contemporary conditions of the study region.

Figure 9 below shows the effect of considering fires in Inland. Top panels (a, b) show the spatial distribution of evergreen trees (tropical and temperate broadleaf trees, and boreal and temperate conifers) biomass. The bottom panels (c, d) show the spatial distribution of grasses (warm and cool grass) biomass. On the left the maps show simulation results without fires, and on the right considering fires. As shown, the simulation of the transition between forests and grasslands in Brazilian Amazonia (approximately highlighted by the dotted ellipsis) is affected by the consideration of fire in the formulation of the model. As simulated, there is an expansion of grasses over forest areas noticeable in the border between the two regions dominated by these types of vegetation.

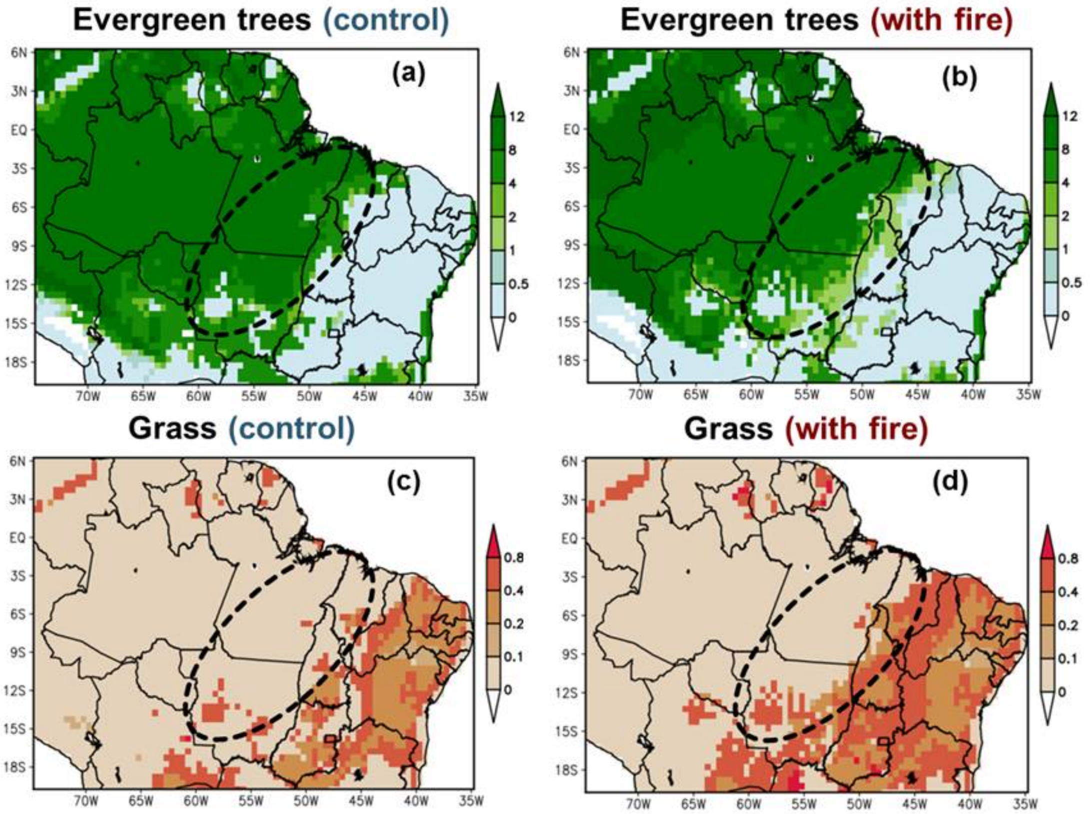

Figure 9: Contemporary distribution of evergreen trees and grasses biomass over the Brazilian Amazonia as simulated by the IBIS-INLAND model. Top panels (a, b) show the spatial distribution of evergreen trees (tropical and temperate broadleaf trees, and boreal and temperate conifers) biomass, and bottom panels (c, d) show the spatial distribution of grasses (warm and cool grass) biomass. On the left the maps show simulation results without fires, and on the right considering fires. The black dotted ellipsis approximately highlights the transition between forests and grasslands in the Brazilian Amazonia.

6.2. BESM-IBIS-INLAND – climatological features

In this section is discussed how the new version of BESM-IBIS-INLAND model can simulate the climatological features. The climate simulation is performed in an ensemble mode, integrating the model with five different initial conditions derived from five consecutive days of NCEP daily analyses, from 01 to 05 December 1960. The results are analyzed for January 1961-December 1990. Ensemble means are used to compare the model results with observational datasets. Global and regional precipitation fields are derived from the Global Precipitation Climatology Project (GPCP, Huffman et al., 1997) and NCEP-NCAR reanalysis (Kalnay et al. 1996) is used to validate the variables in Table 1. The model shows slightly larger values of outgoing long-wave radiation (ROLE) and large values of cloud clover. The mean global precipitation is better simulated than the old version of the model. The model also overestimates the net shortwage radiative flux at the surface and net longwave radiation. The latent heat flux is underestimated by 13 W m^{-2} and can be related with the overestimation of cloud cover. The sensible heat flux is underestimated by 6.5 W

m^{-2}. The analysis indicates that SW radiative transfer code and the cloud cover scheme employed in the model need to be improved.

Table 1 – Ensemble annual global at the top of the atmosphere and surface for: outgoing long-wave radiation (ROLE), cloud cover, precipitataion, precipitable water, sensible heat flux from surface, latent heat flux from surface, net long-wave at ground and net short-wave at bottom. Sign convention is positive for downward flux.

	OBS (NCEP or GPCP)	BESM - old version	BESM-INLAND-IBIS
TOP OF ATMOSPHERE	Global	Global	Global
ROLE (W/m^2)	-231	-239	-239
CLOUD COVER (%)	51	53	70
SURFACE			
Precipitation (mm/day)	2.7	3.5	3.1
Inst.Precipitable Water (mm/day)	23.9	23.9	24.4
Sensible Heat Flux From Surface (W/m^2)	-15.5	-20	-22
Latent Heat Flux Surface (W/m^2)	-82	-102	-95
LW Net at Ground (W/m^2)	-61	-63	-53
SW Net at Bottom (W/m^2)	161	191	177

The main features of the annual precipitation is presented in Figure 10. Over South America there is a deficiency of precipitation over Amazonia and overestimation over Southeast of Brazil. However, especially over Amazonia, this deficiency is lower than the old version of the model. In general, for precipitation, this new version of the model is better than the old version.

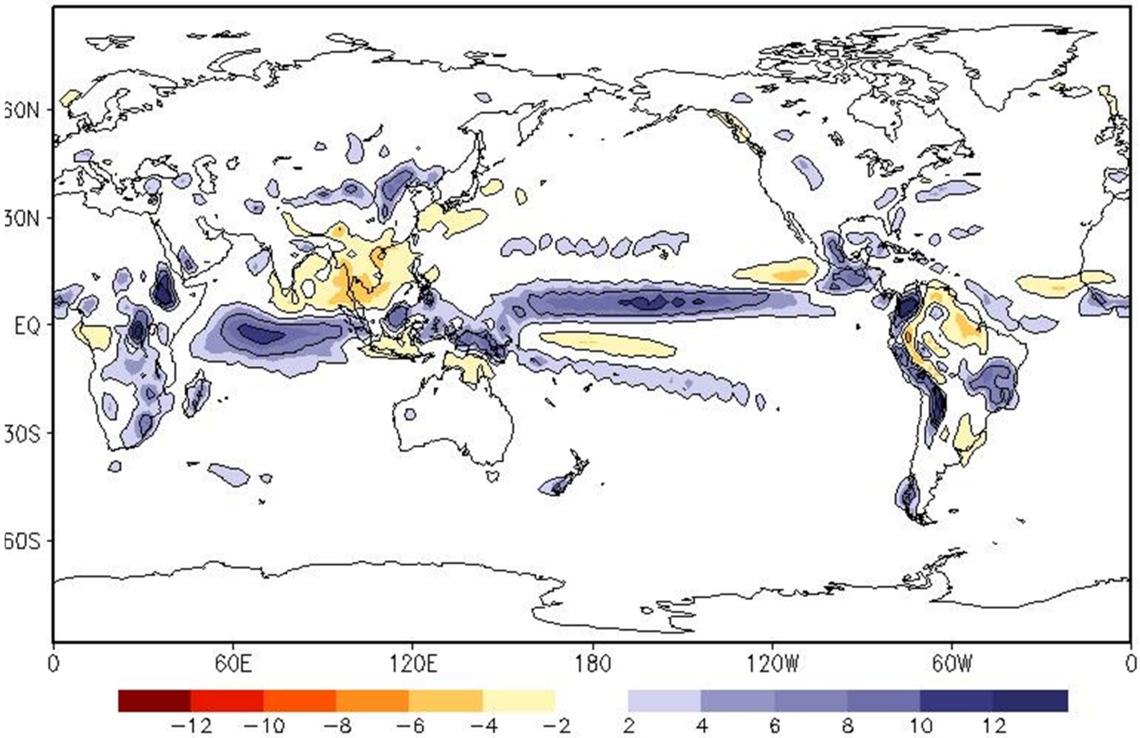

Figure 10 – Climatological precipitation anomalies (mm day $^{-1}$) – difference between model and GPCP.

6.3. HadGEM2-ES

The implementation of HadGEM2-ES in the computational facilities at INPE was considered successful, based on our evaluation of how the model simulated global patterns of variables relevant for fires. For that, we compared long-term average monthly values of atmospheric temperature and specific humidity close to surface, and moisture in the first soil layers, from the model simulations to reference data from other sources of information (Figures 11-13). Model values are from a contemporary climate simulation with HadGEM2-ES forced with climatological sea surface temperatures. Reference data on the selected variables are from the 20th Century Reanalysis (Compo et al. 2011) provided by the NOAA/OAR/ESRL PSD, Boulder, Colorado, USA, from their Web site at http://www.esrl.noaa.gov/psd/.

Generally, the global patterns of temperature, specific humidity, and soil moisture simulated with HadGEM2-ES are similar to the patterns from the reference datasets. The choice of displaying periods for the maps was made based on prevailing wet and dry conditions commonly observed in most of Amazonia in January and September, respectively (Figure 11). As shown, both modelled and reference datasets present seasonal values that generally match expected conditions globally and over the study region. Some differences were also noted. For example, the values of soil moisture from the model (Figure 12c) are somewhat higher than the reference data for most of Amazonia in September. The values of the air temperature near the surface are were also higher for most of Amazonia in January, but generally agree with the reference data for September (Figure 13).

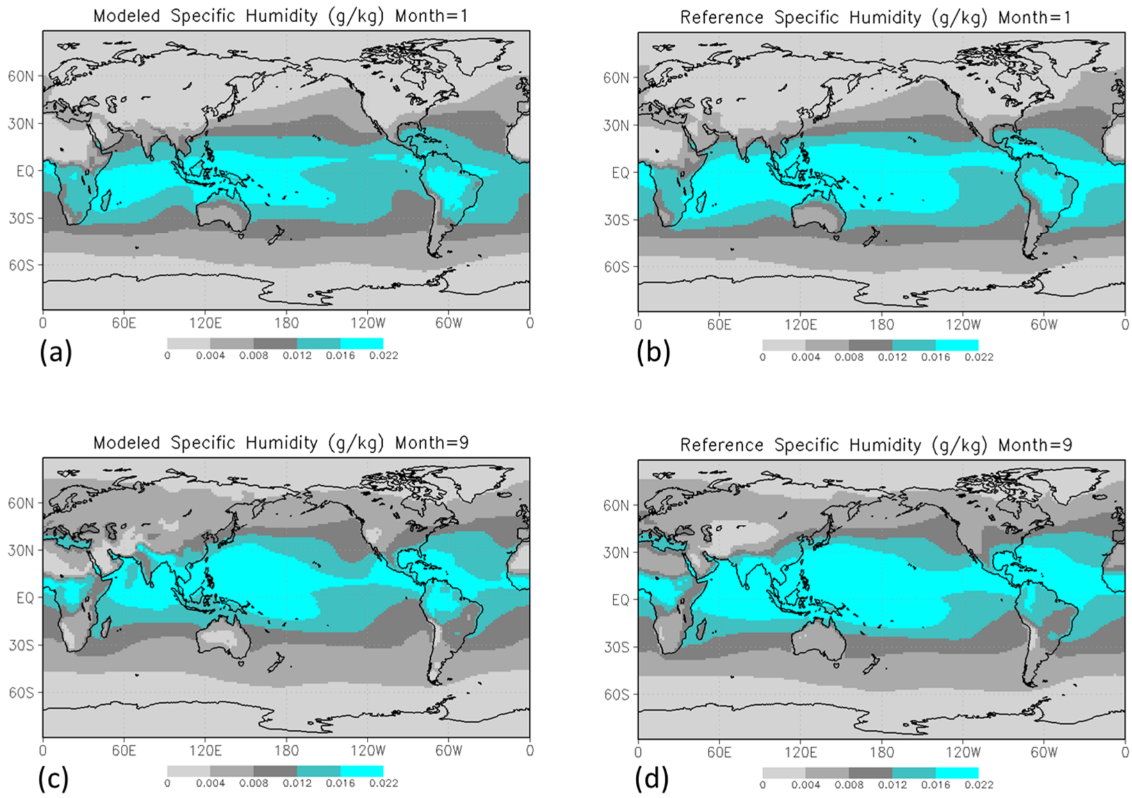

Figure 11 – Global patterns of atmospheric specific humidity near the surface. Top panels show the spatial distribution of the variable for January (Month=1) estimated with HadGEM2-ES (a) and based on the NOAA/OAR/ESRL reanalysis (b). Bottom panels show its spatial distribution for September (Month=9) estimated with HadGEM2-ES (c) and based on the NOAA/OAR/ESRL reanalysis (d).

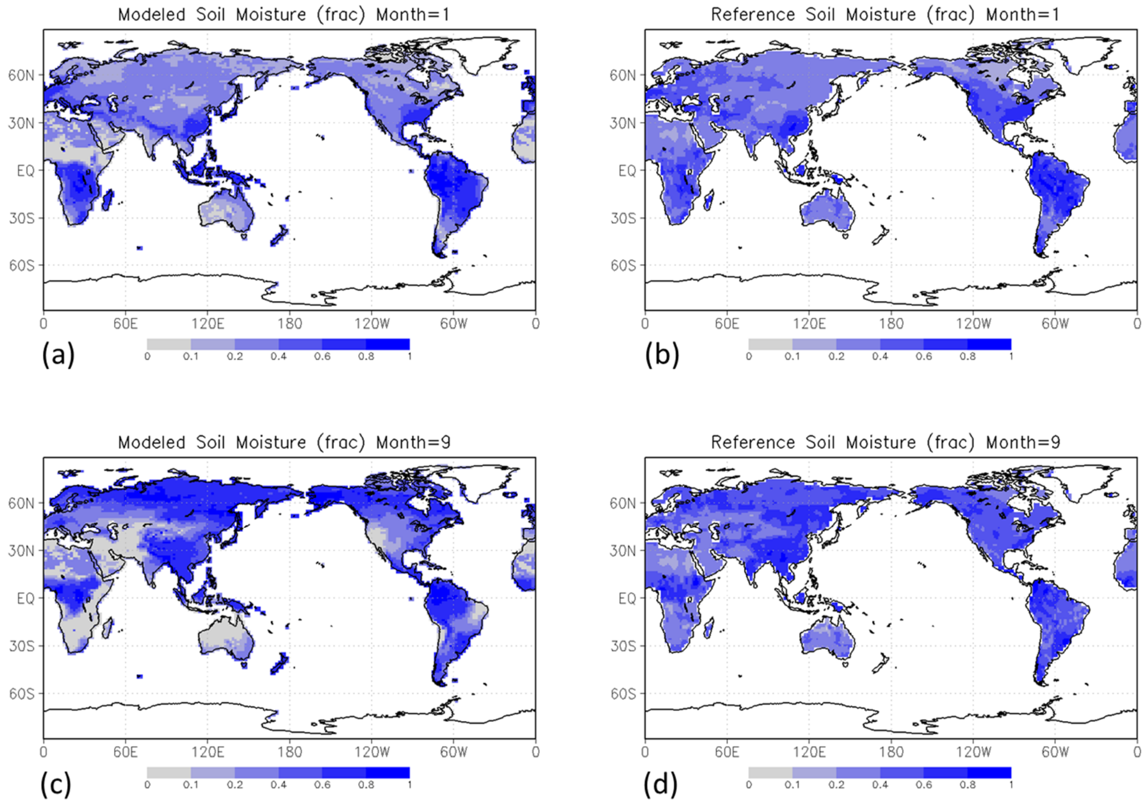

Figure 12 – Global patterns of soil moisture in the first soil layers. Top panels show the spatial distribution of the variable for January (Month=1) estimated with HadGEM2-ES (a) and based on the NOAA/OAR/ESRL reanalysis (b). Bottom panels show its spatial distribution for September (Month=9) estimated with HadGEM2-ES (c) and based on the NOAA/OAR/ESRL reanalysis (d).

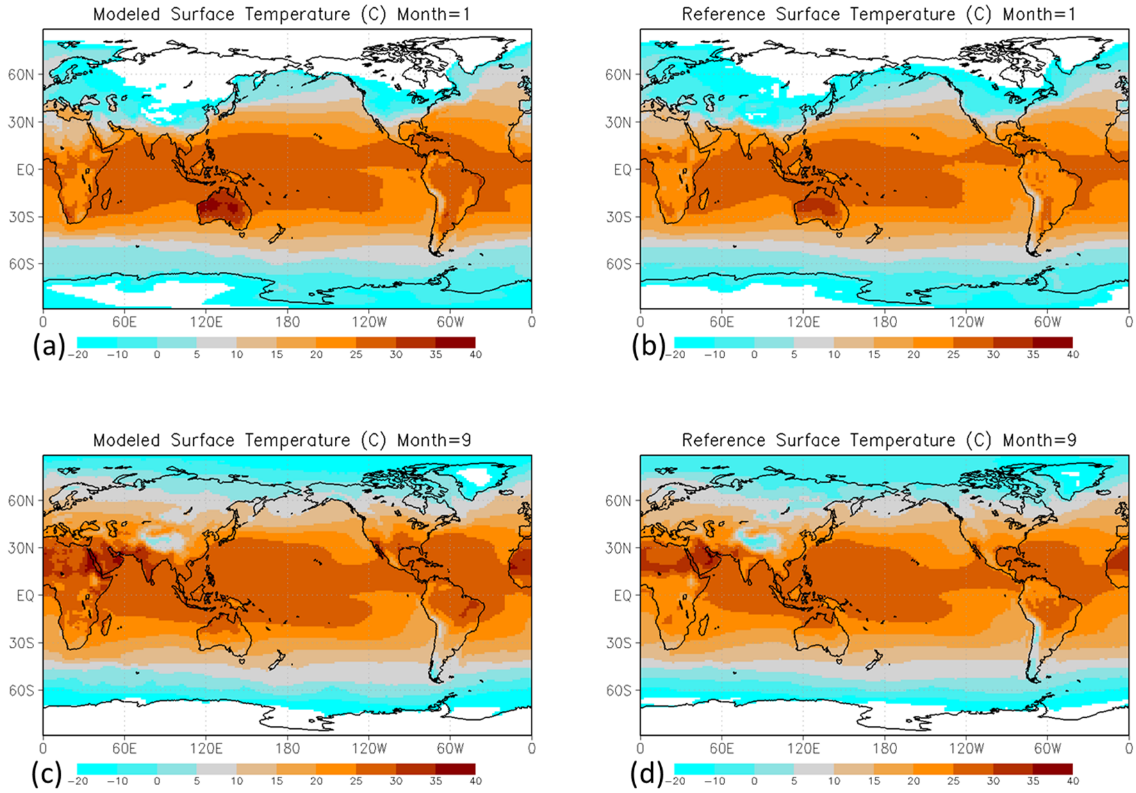

Figure 13 – Global patterns of air tmospheric specific humidity near the surface. Top panels show the spatial distribution of the variable for January (Month=1) estimated with HadGEM2-ES (a) and based on the NOAA/OAR/ESRL reanalysis (b). Bottom panels show its spatial distribution for September (Month=9) estimated with HadGEM2-ES (c) and based on the NOAA/OAR/ESRL reanalysis (d).

The implementation of fire equations by Kasikowski et al. in HadGEM2-ES was tested by comparing the model's offline estimation of burning extent to the burned area from the reference GFED database (Figure 14 and Figure 15). As show by these figures, the model was able to reproduce the large-scale fire patterns. Maps of global estimation of burned area show similar spatial patterns between modelled (Figure 14a and c) and observed (Figure 14b and d) burned area in January and September 2005. The time series of spatial averages also display model values that are within the ranges determined by the observations (Figure 15), with cases where timing is also correct, mainly in the SH Tropics (d) and most of 2004-2005 in South America (c).

There are, however, differences between the model and observed values. One can note, for example, important overestimation of low values and underestimation of high values, and lower variability in modelled results. As shown, there is an overspread non-zero background values in South America and Australia, and in desert areas of Africa. In South America, there is large overestimation of burned area in the North and Northeast of the continent, and underestimation in central areas. In Africa, there is overestimation of values in forest areas, but the positions of maximum values are generally correct.

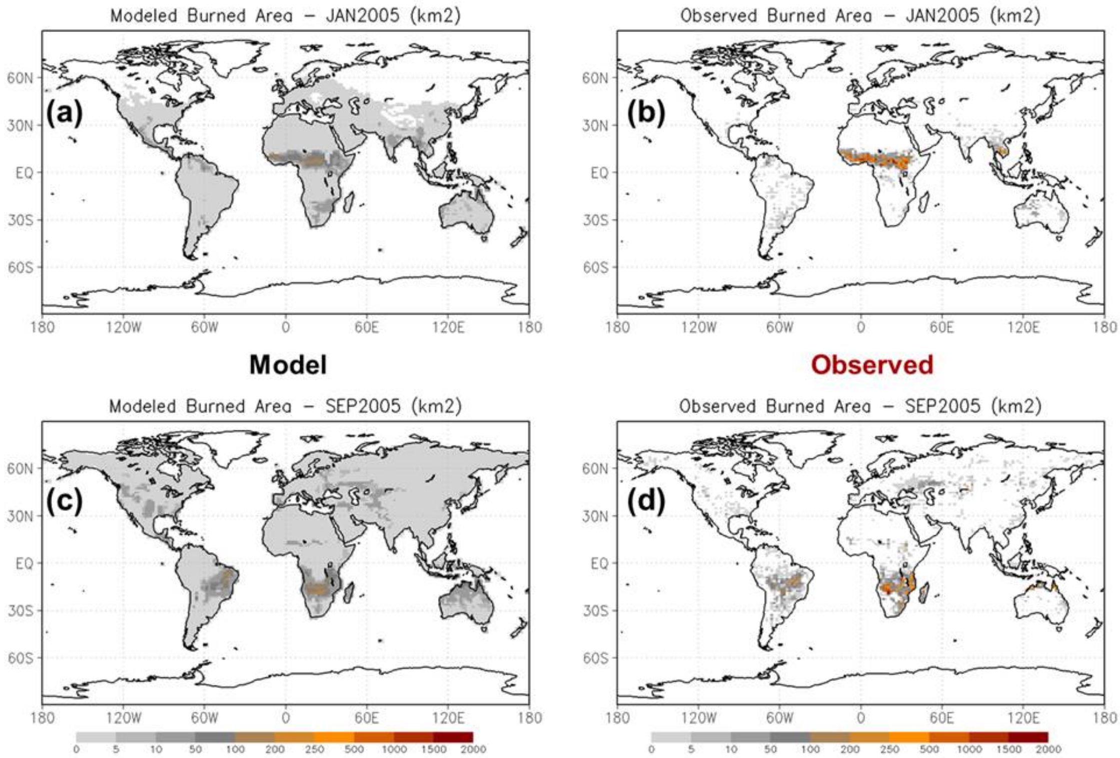

Figure 14: Global patterns of burned area for year 2005. Top panels show the spatial distribution of burned area for January 2005 estimated with HadGEM2-ES (a) and based on the GFED database (b). Bottom panels show the spatial distribution of burned area for September 2005 estimated with HadGEM2-ES (c) and based on the GFED database (d).

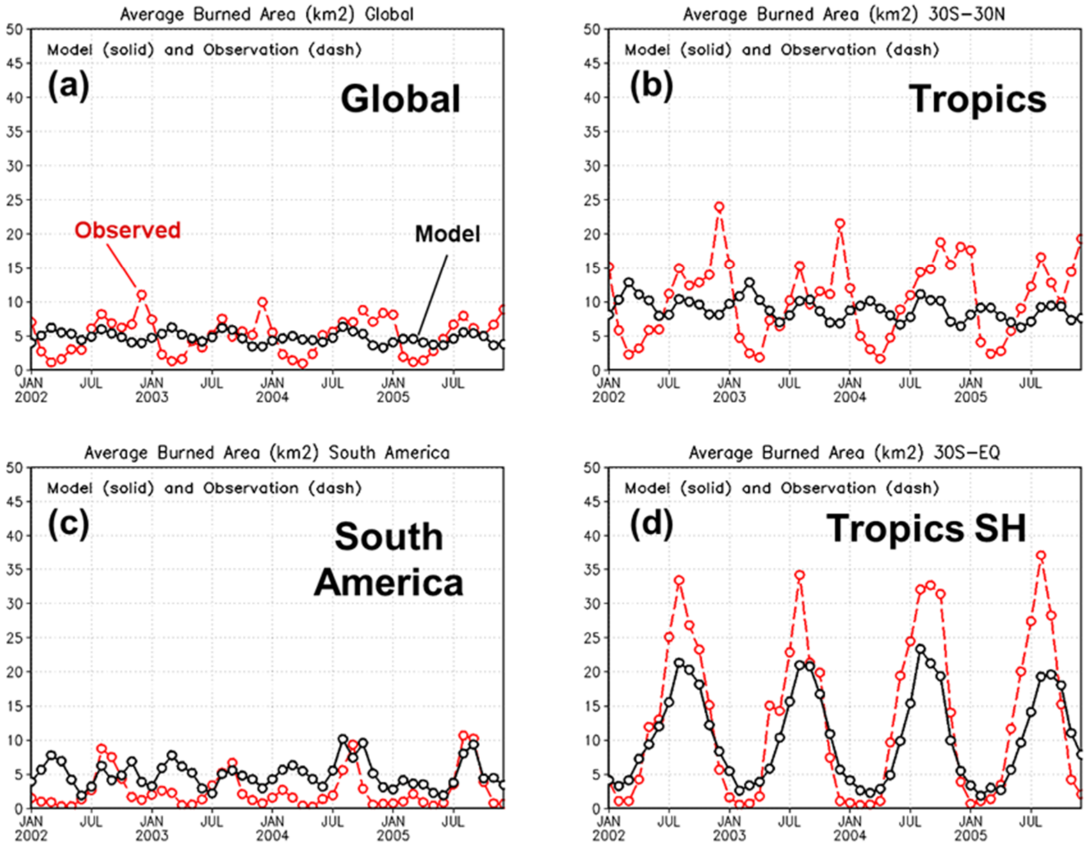

Figure 15: Time series of average burned area from 2002 to 2005. Values for the globe in (a), for the Tropics in (b), for South America in (c), and for Southern Hemisphere Tropics in (d). In black are values estimated with the fire model in HadGEM2-ES, and in red values from the GFED database.

7. Simulations of fire and effects on climate

To evaluate the effects of fires in combination with climate change and deforestation, the BESM with IBIS-INLAND was run under greenhouse gas concentrations corresponding to historical conditions and RCPs 4.5 and 8.5 (van Vuuren et al. 2011). The simulations were prepared in two main categories:

1) The model was running under historical and RCPs greenhouse gas concentration, and
2) the model was forced by the same configuration as in 1 but also considering the effects of deforestation (scenario C, as described in Section 4) and forest fire (as described in Section 3).

The model simulations were planned for a total of 140 years (from 1961 to 2100). There was an initial spin-up of 50 years (from 1961-2005) with increased prescribed atmospheric CO_2 concentrations (from 317 to 378 ppm) and from 2006 up to 2100 with increased atmospheric CO_2 concentrations under RCPs greenhouse gas concentration.

7.1. BESM - RCP4.5

The results for the response of BESM model with IBIS-INLAND under RCP4.5 for the period 2065-2070 show that the impacts increase when the effects of fires and land-use change are combined, and changes in the east/northeast and south of Amazonia are potentially stronger.

The results show warmer air temperature near the surface in all cases compared to the control case, and in some areas the warming is about 2-3°C (Figure 16). From the evaluation of climate change only, there is also indication of increase in annual precipitation in the south, with small change in the rest of the region (Figure 17). When considering deforestation and fires, the spatial patterns of the changes are the same, but the indication of decrease in annual precipitation becomes more noticeable in the north. The reduction in precipitation occurs mainly during the dry season (June-November) in both cases, and there is an increase in the length of the dry season (Figure 18).

In the simulation considering only the climate change we can see an increase of upper-canopy biomass (Figure 19a and b), likely related to CO_2 fertilization. When all factors are considered, there is reduction of upper-canopy biomass and an increase of lower-canopy biomass, indicating a shift from forest to grasses (Figure 19c and d).

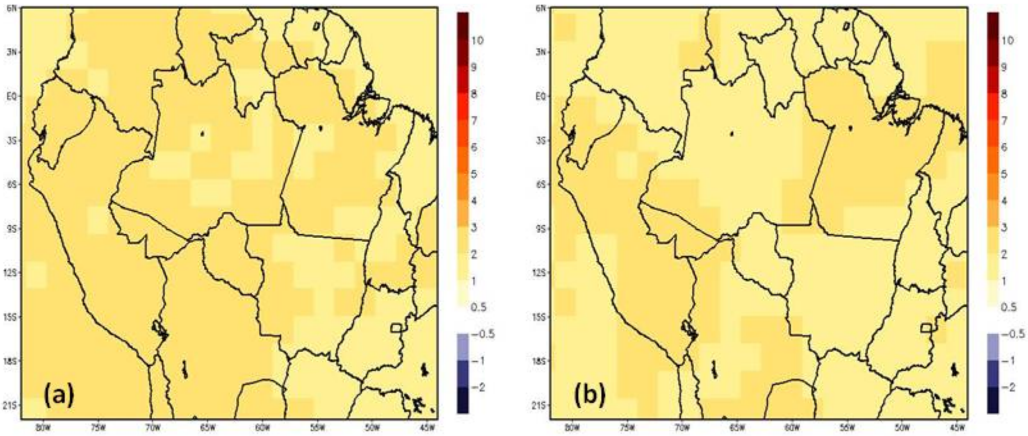

Figure 16: Mean annual temperature anomalies (°C) compared to the control for 2065-2070: (a) the model was run under RCP4.5 greenhouse gas concentration, (b) as (a) but also considering the effects of deforestation and forest fire.

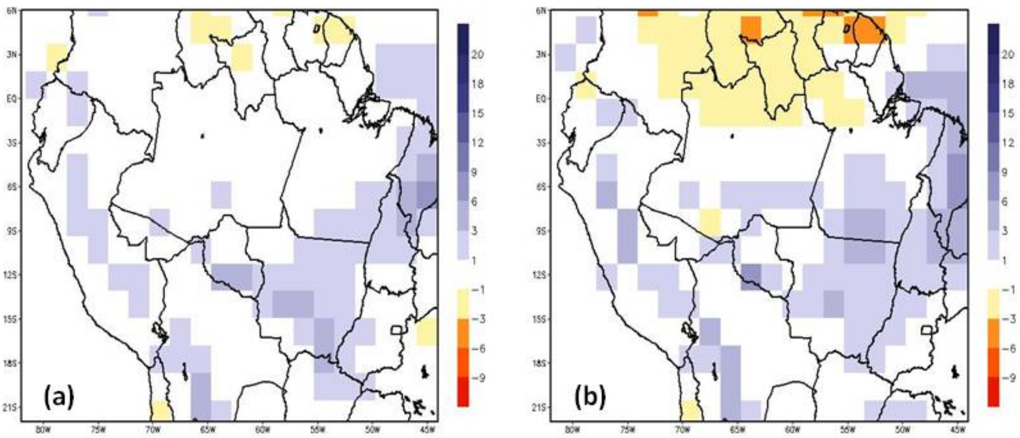

Figure 17: Mean annual precipitation anomalies (mm/day) compared to the control for 2065-2070: (a) the model was run under RCP4.5 greenhouse gas concentration, (b) as (a) but also considering the effects of deforestation and forest fire.

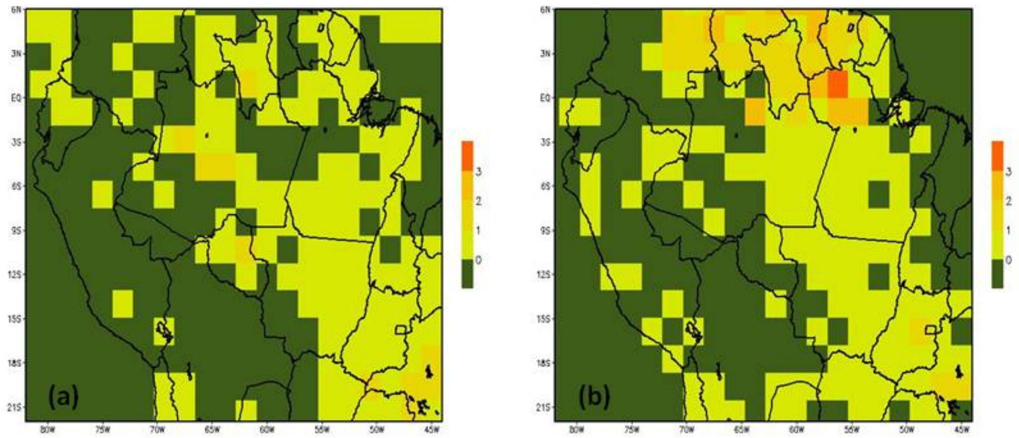

Figure 18: Dry season length anomalies (months) compared to the control for 2065-2070: (a) the model was run under RCP4.5 greenhouse gas concentration, (b) as (a) but also considering the effects of deforestation and forest fire.

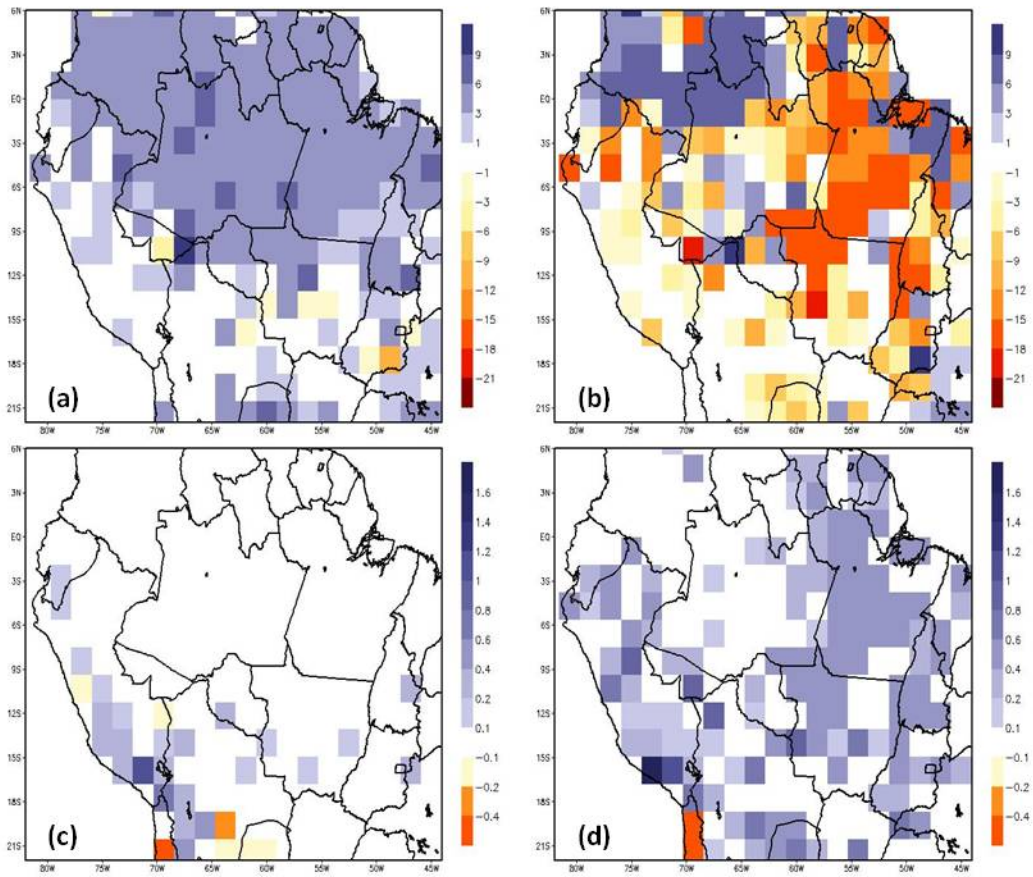

Figure 19: Biomass anomalies (KgC/m^2) of the upper canopy (a and b) and biomass anomalies of the lower canopy (c and d) compared to the control for 2065-2070: (a) and (c) the model was run under RCP4.5 greenhouse gas concentrations, (b) and (d): as (a) and (c) but also considering the effects of deforestation and forest fire.

According to these estimates, combining fire with changes in land-use and climate under RCP4.5 may be important for Amazonia. Important effects include increase in surface temperature, decrease in precipitation and evapotranspiration, increase in dry season length and reduction of upper-canopy biomass. These changes are also associated with increase of the biomass of grasses and seasonal forest and savanna, and decrease of tropical forest. We note that these analyses were concentrated in the combined effects of the changes in climate and human activities, and did not evaluate the relative strength of each of these factors. For example, we did not evaluate how much of the projected changes in biomass are due to direct land use or how much is from fire.

7.2. BESM – RCP8.5

The results of the response of BESM with IBIS-INLAND under RCP8.5 also show that impacts increase when the effects of land use changes and fire are incorporated (Figure 20-23). Important changes were identified in the East/Northeast and South of the Amazonia and were more evident when the effects of climate change and fire are considered. It is important to note that we expected that the stronger effects would be observed when including land use. The results, however, showed relatively small impacts of land use. We note that these results need further investigation, and consider the possibility of a wrong treatment of the land use scenarios in the model.

The results currently show warmer near-surface air temperature in all cases compared to the control case, and in some areas the warming is about 2-3^{o}C (Figure 20). This relative warming of the deforested land surface is consistent with the lower leaf area and the lower surface roughness length (not showed here). The BESM model simulates a positive annual precipitation trend in response to the standard RCP8.5 forcing (Figure 21a) and when are considered all effects (Figure 21c). There is a reduction in annual precipitation when are considered the effects of climate change and fire mainly over eastern/northeastern Amazonia and increase in the southeast (Figure 21b). The reduction in precipitation is more evident when are considered the effects of climate change and fire (Figure 21b). The reduction in precipitation occurs mainly during the dry season (June-November), and there is an increase in dry season length that is more evident when are considered the effects of climate change and fire (Figure 22b). As discussed in Section 4, in regions marked by a short dry season, i.e. where conditions are wetter, the effect of deforestation and forest fire on ET is much smaller than in regions where there is a long dry season.

In the simulation considering only climate change we can see an increase of upper-canopy biomass (Figure 23a). However, when all effects are considered, there is a reduction of upper-canopy biomass and an increase of the biomass in grasses (Figure 23b,c,e,f). Thus, there is indication that the combination of climate change, deforestation and potential for higher fire occurrence may lead to important impacts that add to the vulnerability of forests mainly in the East/Northeast and South of the Amazonia.

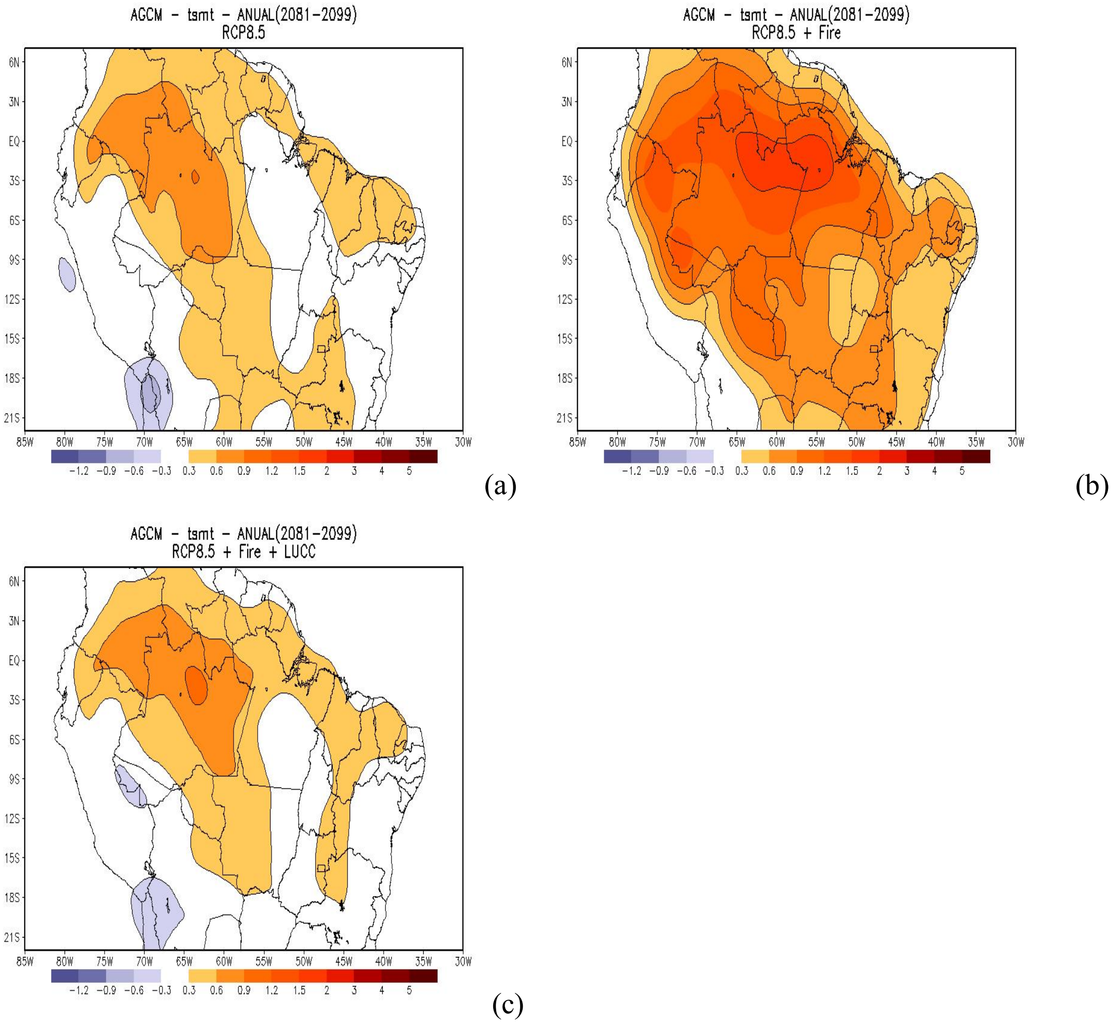

Figure 20. Mean annual temperature anomalies (ºC) compared to the control for 2081-2099: (a) the model was run under RCP8.5 greenhouse gas concentration, (b) the model was forced by the same configuration in (a) but also considering the effects of forest fire, and (c) the model was forced by the same configuration in (a) but also considering the effects of deforestation and forest fire.

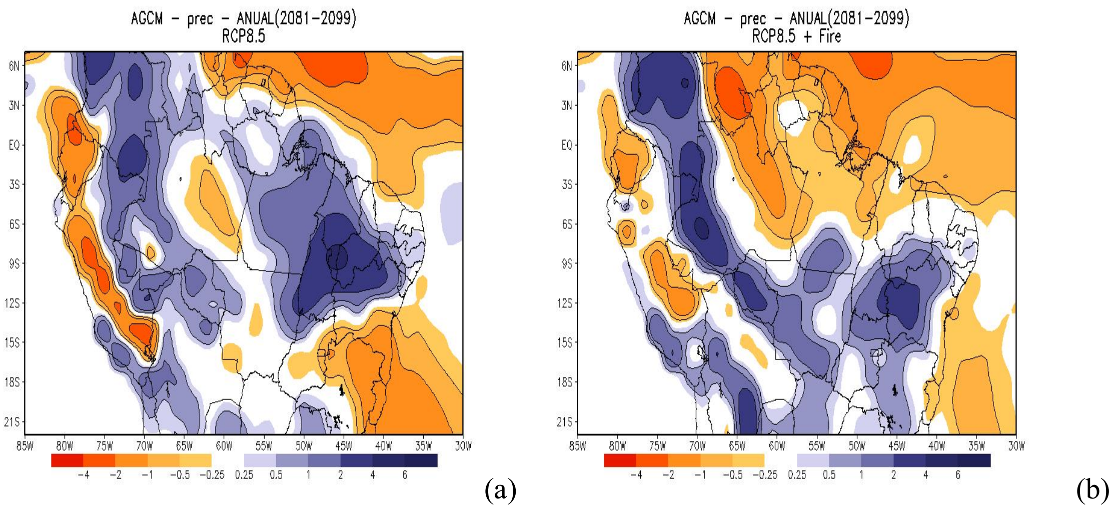

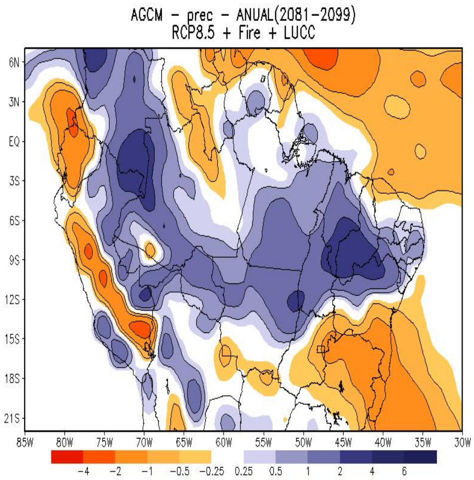

(c)

Figure 21. Mean annual precipitation anomalies (mm/day) compared to the control for 2081-2099: (a) the model was run under RCP8.5 greenhouse gas concentration, (b) the model was forced by the same configuration in (a) but also considering the effects of forest fire, and (c) the model was forced by the same configuration in (a) but also considering the effects of deforestation and forest fire.

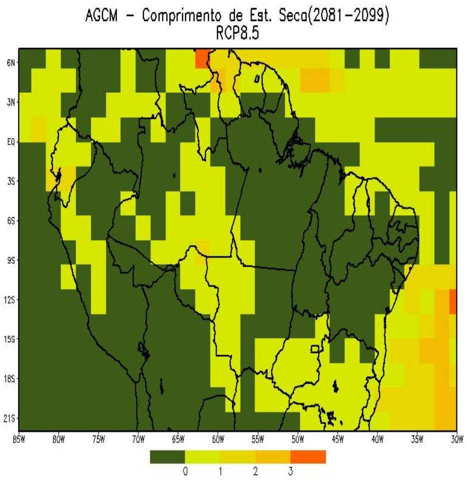

(a)

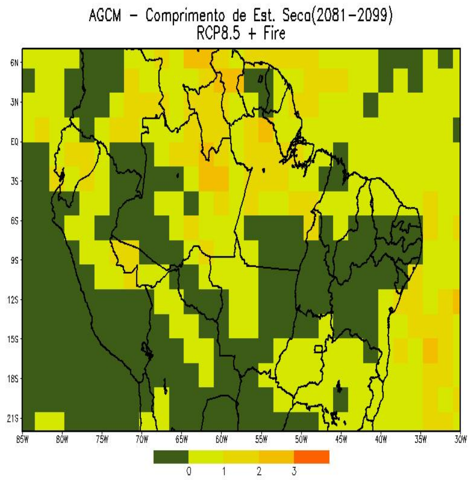

(b)

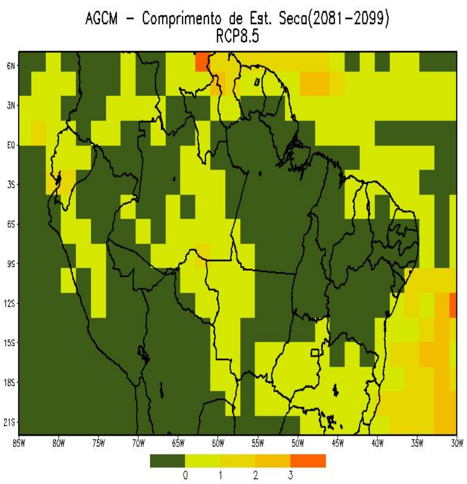

(c)

Figure 22. Dry season length anomalies (months) compared to the control for 2081-2099: (a) the model was run under RCP8.5 greenhouse gas concentration, (b) the model was forced byt the same configuration in (a) but also considering the effects of forest fire, and (c) the model was forced by the same configuration in (a) but also considering the effects of deforestation and forest fire.

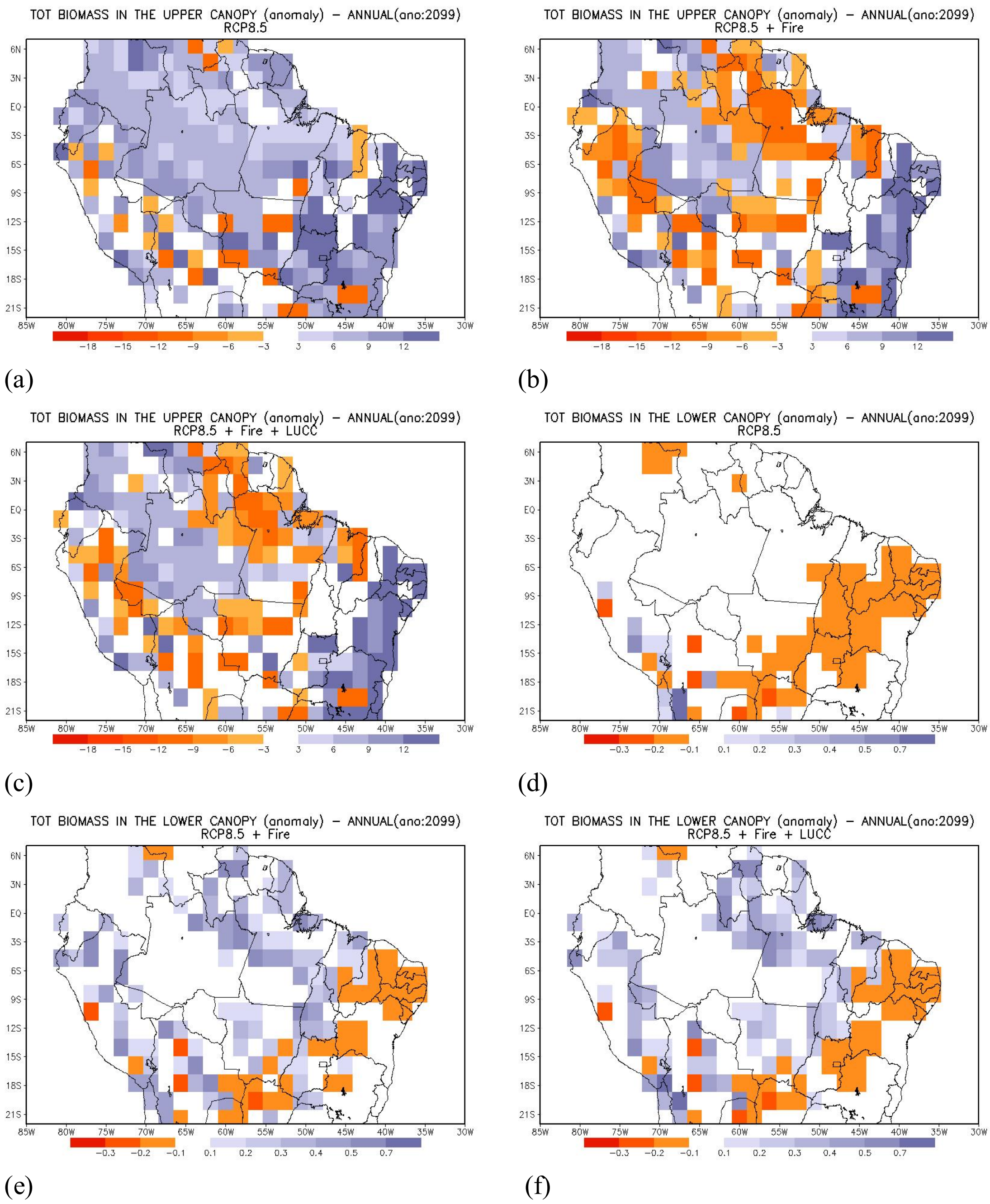

Figure 23. Biomass anomalies (KgC/m^2) of the upper canopy (a, b, c) and biomass anomalies of the lower canopy (d, e and f) compared to the control for 2081-2099: (a) and (d) the model was run under RCP8.5 greenhouse gas concentrations, (b) and (d): as (a) and (c) but also considering the effects of forest fire, (e) and (f): as (a) and (c) but also considering the effects of deforestation and forest fire.

In summary, the results indicate that important changes may occur in the East/Northeast of the Amazon, with an increase in surface temperature, and decrease in precipitation and evapotranspiration (not showed here), an increase in dry season length and a reduction of upper-canopy biomass and an increase of the biomass in grasses, suggesting replacement of tropical forest by seasonal forest and/or savanna (not showed here). The effects of fire and land use cover change and climate changes, resulting in warmer and possibly drier climates in some portions of Amazonia may be important to the future of biome distribution in the region. The vulnerability of Amazon rainforest to more frequent and severe droughts, either through a direct effect on tree mortality or through an indirect effect, via increased probability of vegetation fires, is important to understand the potential for an Amazon forest dieback and its implications for the global carbon cycle and future climate.

8. Summary

This deliverable reports the incorporation of fire into Earth system models and the impacts on climate. Fire models are important tools for synthesis and projections, reflecting the knowledge obtained from observations made on the ground or by satellites, and enabling the evaluation of future fires in response to scenarios of land surface and climate.

The fire model implemented in HadGEM2-ES is based on the work of Kasikowski et al., initially designed for HadCM3. The model estimates burned area soil and atmospheric moisture, assuming constant rates of ignition. The new fire equations were able to reproduce large-scale fire patterns, with spatial and temporal features that are similar to the patterns determined with remote sensing. In South America, there is overestimation of burned area in the North and Northeast of the continent, and underestimation in central areas. Feedbacks between fire occurrence and vegetation dynamics are not currently implemented, but only offline estimation of burning extent.

The BESM with IBIS-INLAND has been improved to represent the major features of the fire occurrence with emphasis on the ecosystems in Brazil, based on the method by Arora and Boer (2005). At this stage, the development and implementation of the fire model is concentrated on the simulation of fire probability and effects on vegetation dynamics only. For that, we implemented the fire occurrence probability equations, where fire potential is driven by the combination of presence of fuel, flammability, and sources of ignition.

To evaluate the effects of fires in combination with climate change and deforestation, the BESM with IBIS-INLAND was run under greenhouse gas concentrations corresponding to historical conditions and RCPs 4.5 and 8.5. According to the simulated results, combining fire with changes in land-use and climate may be important for Amazonia. The major changes were estimated in the eastern and southern portions of the basin, with an increase in surface temperature, decrease in precipitation, increase in dry season length and reduction of upper-canopy biomass. These changes are also associated with increase of biomass of grasses and decrease of forest biomass.

We expected that the results from BESM with IBIS-INLAND would present progressively stronger effects when considering changes in climate, deforestation, and fires, respectively. The results, however, show relatively small impacts of deforestation and a pronounced effect of fire. To our knowledge, these features are counterintuitive, and we plan to further investigate the sensitivity of the model to these factors and re-evaluate our treatment of the land-use scenarios in the model. We also note that these analyses were concentrated in the combined effects of fires, climate change and land use, and did not evaluate the relative strength of each of these factors, which is also a subject for further research.

9. References

Andreae M.O., Merlet P. (2001) Emissions of trace gases and aerosols from biomass burning. Global Biogeochemical Cycles, 15, 955-966.

Arora VK, Boer GJ (2005) Fire as an interactive component of dynamic vegetation models. Journal of Geophisycal research, vol 110, doi:10.1029/2005JG000042.

Boisier et al. Projected strengthening of Amazonian dry season by constrained climate model simulations. Submitted to Nature Climate Change.

Cardoso MF, Hurtt GC, Moore B, Nobre CA, Bain H (2005). Field work and statistical analyses for enhanced interpretation of satellite fire data. Remote Sensing of Environment, 96, 212–227. DOI:10.1016/j.rse.2005.02.008.

Cardoso, M.F., Hurtt, G.C., Moore III, B., Nobre, C.A., & Prins, E.M. (2003). Projecting future fire activity in Amazonia, Global Change Biology, 9, 656-669.

Cochrane, M.A. (2003). Fire science for rainforests, Nature, 421, 913-919.

Cochrane, M.A., Schulze, M.D. (1999). Fire as a recurrent event in tropical forests of the eastern Amazon: effects on forest structure, biomass, and species composition. Biotropica, 31(1), 1-16.

Collins, W. J., and Coauthors (2011) Development and evaluation of an Earth-System model-HadGEM2. Geosci Model Dev, 4, 1051-1075.

Compo, G.P., J.S. Whitaker, P.D. Sardeshmukh, N. Matsui, R.J. Allan, X. Yin, B.E. Gleason, R.S. Vose, G. Rutledge, P. Bessemoulin, S. Brönnimann, M. Brunet, R.I. Crouthamel, A.N. Grant, P.Y. Groisman, P.D. Jones, M. Kruk, A.C. Kruger, G.J. Marshall, M. Maugeri, H.Y. Mok, Ø. Nordli, T.F. Ross, R.M. Trigo, X.L. Wang, S.D. Woodruff, and S.J. Worley (2011) The Twentieth Century Reanalysis Project. Quarterly J. Roy. Meteorol. Soc., 137, 1-28. DOI: 10.1002/qj.776.

Foley, J.A., I.C. Prentice, N. Ramankutty, S. Levis, D. Pollard, S. Sitch, and A. Haxeltine (1996). An integrated biosphere model of land surface processes, terrestrial carbon balance, and vegetation dynamics. Global Biogeochemical Cycles 10(4), 603-628.

Giglio L (2013) MODIS Collection 5 Active Fire Product User's Guide, Version 2.5. Department of Geographical Sciences, University of Maryland. http://modis-fire.umd.edu/Documents/MODIS_Fire_Users_Guide_2.5.pdf.

Good P. et al. (2011) Quantifying environmental drivers of future tropical forest extent. J Climate 24, 1337–1349

Good, P. et al. (2013) Comparing tropical forest projections from two generations of Hadley Centre Earth System models, HadGEM2-ES and HadCM3LC. J Climate 26, 2, 495–511. doi:10.1175/jcli-d-11-00366.1

Golding, N., and R. Betts (2008) Fire risk in Amazonia due to climate change in the HadCM3 climate model: Potential interactions with deforestation. Global Biogeochem. Cycles, 22, Gb4007.

Huffman G.J., Adler R.F., Arkin P., Chang A., Ferraro R., Gruber A., Janowiak J., McNab A., Rudolf B., Schneider U. (1997). The global precipitation climatology project (GPCP) combined precipitation dataset. *Bulletin of the American Meteorological Society* **78**: 5-20.

Hughes, R.F., Kauffman, J.B., Cummings, D.L. (2000) Fire in the Brazilian Amazon: 3. Dynamics of biomass, C, and nutrient pools in regenerating forests. Oecologia, 124,574-588.

INPE 2014: Monitoring of vegetation fires with satellites in near real-time: Statistics – Brazil. Accessed 13 Nov 2014 <http://www.inpe.br/queimadas/estatisticas.php>

Joetzjer, E. et al., 2013: Present-day and future Amazonian precipitation in global climate models: CMIP5 versus CMIP3, Clim. Dynam., 41, 2921–2936, doi:10.1007/s00382-012-1644-1.

Kasikowski T, Venevsky S, Falloon P, Poulter B, Betts R, Boucher O, Golding N. Development and optimisation of a scheme for simulating burnt area in a climate model. In preparation.

Kalnay, E., and Coauthors, 1996: The NCEP/NCAR 40-Year Reanalysis Project. Bull. Amer. Meteor. Soc., 77, 437–471.

Kaufman, Y.J., Fraser, R.S. (1997) The effect of smoke particles on clouds and climate forcing. Science, 277, 1636-1639.

Kauffman, J.B., Cummings, D.L., Ward (1998) Fire in the Brazilian Amazon: 2. Biomass, nutrient pools, and losses in cattle pastures. Oecologia, 113: 415-427.

Kucharik, C.J., J.A. Foley, C. Delire, V.A. Fisher, M.T. Coe, J. Lenters, C. Young-Molling, N. Ramankutty, J.M. Norman, and S.T. Gower (2000). Testing the performance of a dynamic global ecosystem model: Water balance, carbon balance and vegetation structure. Global Biogeochemical Cycles 14(3), 795-825.

Nepstad D.C., Verissimo, A., Alencar, A.A. et al. (1999). Large-scale impoverishment of Amazonian forests by logging and fire. Nature 98, 505-508.

Nobre P., Siqueira L., Almeida R., Malagutti M., Giarolla E., Castelão G., Bottino M., Kubota P., Figueroa S., Costa M., Baptista M., Irber L., Marcondes G. (2013) Climate Simulation and Change in the Brazilian Climate Model. J. Climate, 26, 6716\u20136732. doi: http://dx.doi.org/10.1175/JCLI-D-12-00580.1

Pruppacher H., and Klett J. (1980) Microphysics of Clouds and Precipitation. Nature, 284 (5751), 88-88.

Taylor, K. E., R. J. Stouffer, and G. A. Meehl, 2012: An Overview of CMIP5 and the Experiment Design. Bull. Am. Meteorol. Soc., 93, 485-498.

G. R. van der Werf, J. T. Randerson, L. Giglio, G. J. Collatz, M. Mu, P. S. Kasibhatla, D. C. Morton R. S. DeFries, Y. Jin, e T. T. van Leeuwen (2010) Global fire emissions and the contribution of deforestation, savanna, forest, agricultural, and peat fires (1997 - 2009) Atmos. Chem. Phys. Discuss., 10, 16153–16230.

Schroeder W., Prins E., Giglio L., Csiszar I., Schmidt C., Morisette J., Morton D. (2008) Validation of GOES and MODIS active fire detection products using ASTER and ETM+ data, Remote Sensing of Environment, doi:10.1016/j.rse.2008.01.005.

Sombroek, W., 2001: Spatial and temporal patterns of Amazonian rainfall: consequences for the planning of agricultural occupation and the protection of primary forests. Ambio, 30, 388–396.

van Vuuren, D. P., and Coauthors, 2011: The representative concentration pathways: an overview. Climatic Change, 109, 5-31.